

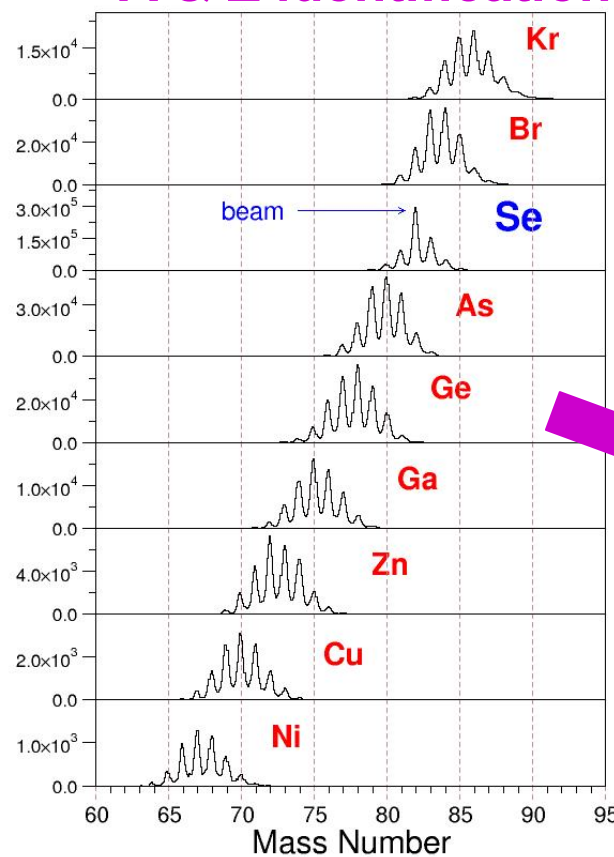
First results of the CLARA – PRISMA setup installed at LNL

A.Gadea INFN-LNL Legnaro

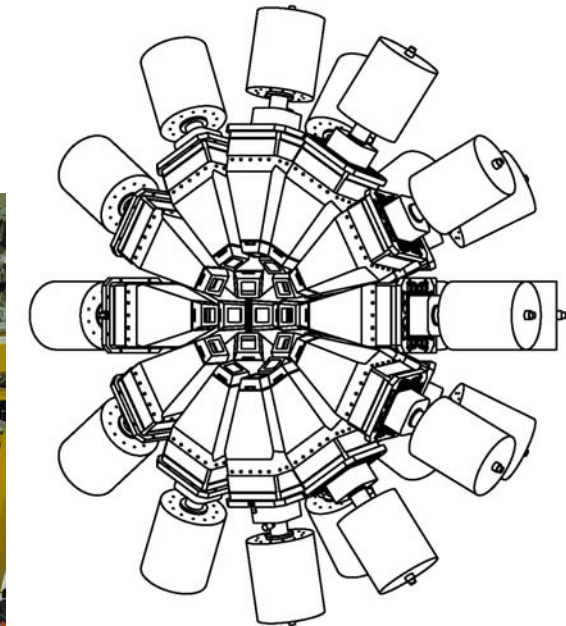
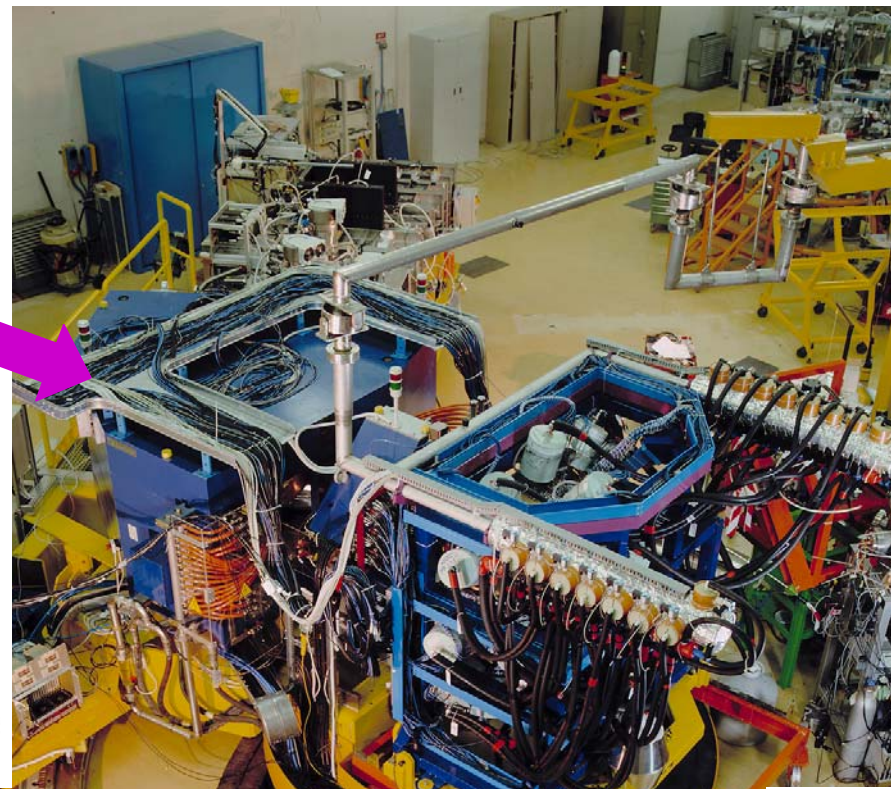
**Gamma Spectroscopy in products of binary reactions
with the “intense” stable beams from the LNL
Tandem-ALPI (present) and PIAVE-ALPI (future)**

- **Moderately neutron rich nuclei produced by Multi-nucleon transfer or deep inelastic collisions**
- **Non-Yrast states populated in quasi-elastic reactions**

A & Z identification

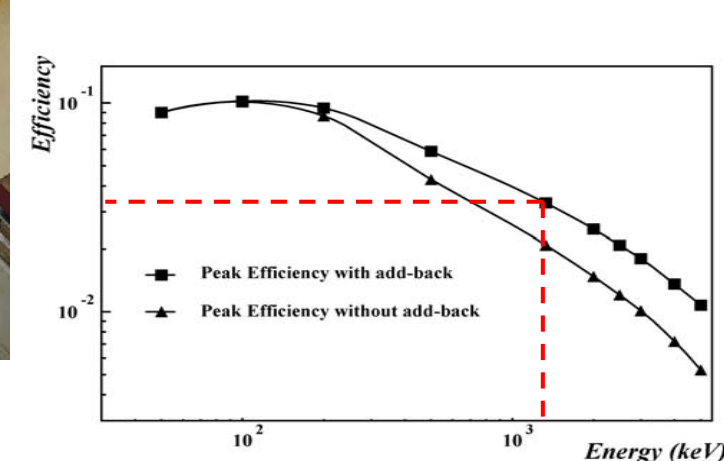
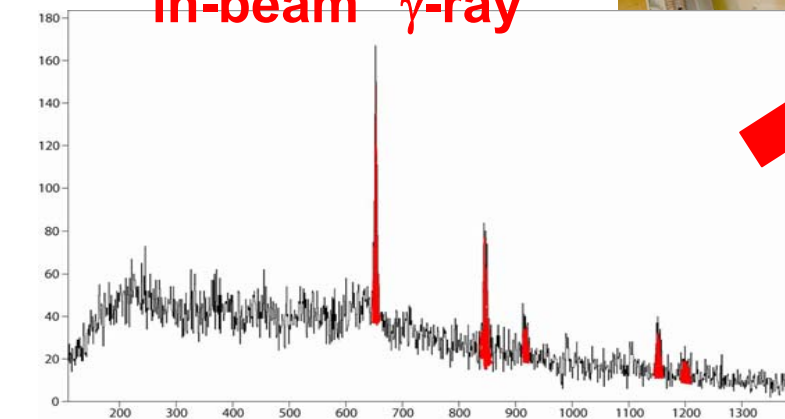


CLARA-PRISMA setup

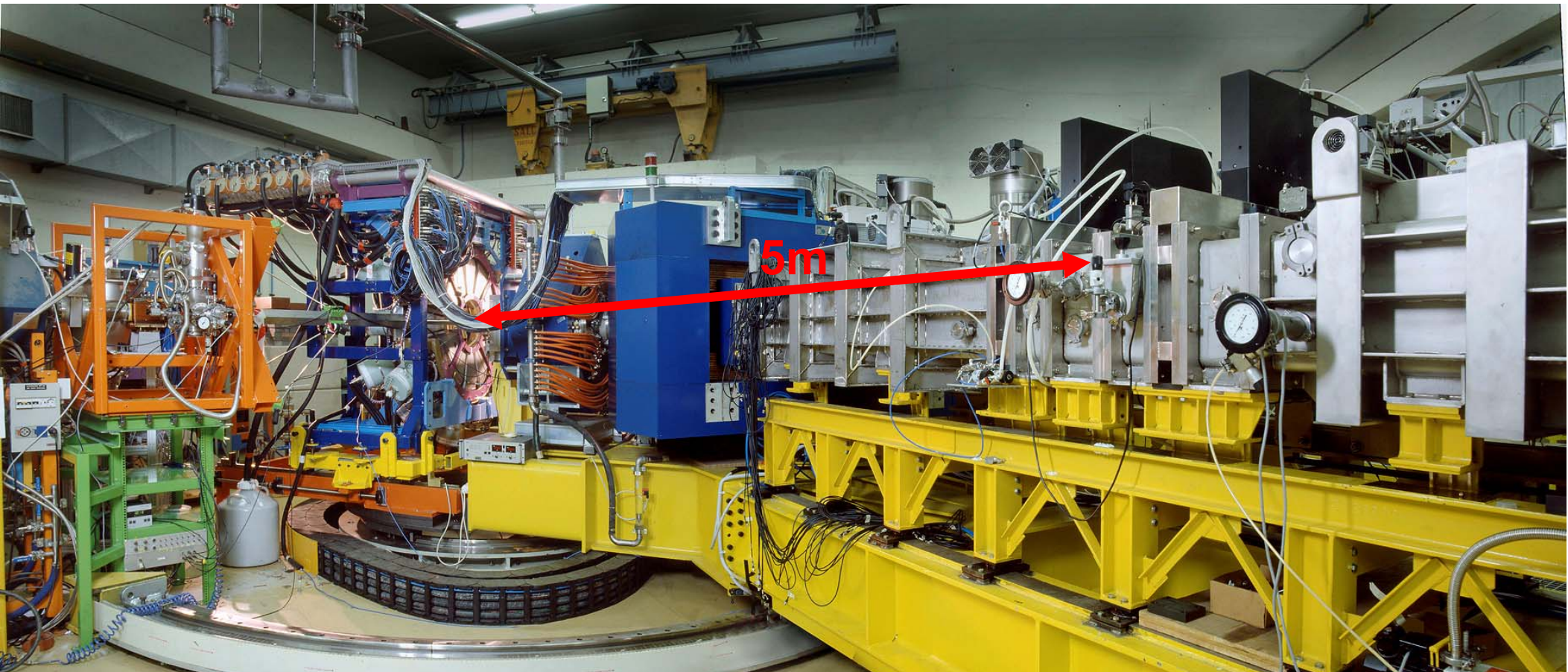


**25 Euroball Clover detectors
for $E\gamma = 1.3\text{MeV}$**
Efficiency $\sim 3\%$
Peak/Total $\sim 45\%$
FWHM $\sim 10\text{ keV}$
(at $v/c = 10\%$)

“in-beam” γ -ray



CLARA-PRISMA setup



PRISMA: Large acceptance Magnetic Spectrometer

$\Omega = 80 \text{ msr}$

$\Delta Z/Z \approx 1/60$ (Measured)

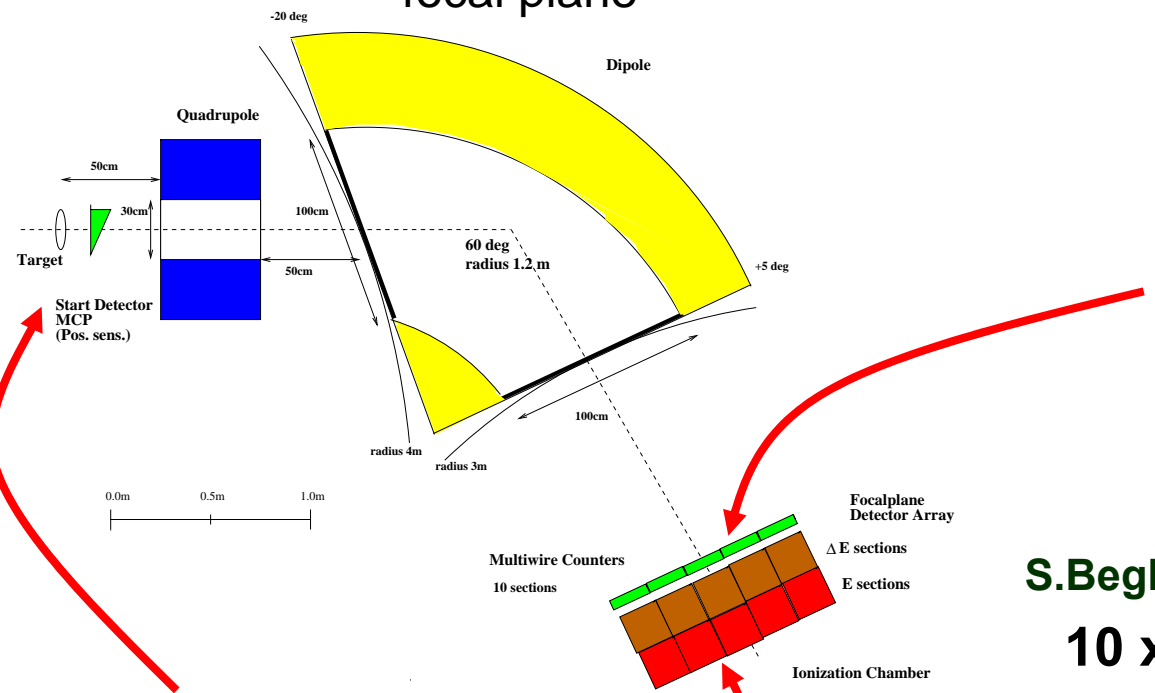
$\Delta A/A \approx 1/190$ (Measured)

Energy acceptance $\pm 20\%$

$B_p = 1.2 \text{ T.m}$

The PRISMA Spectrometer Detectors

Large dispersion dipole: 4cm / % at the focal plane



Position sensitive MCP



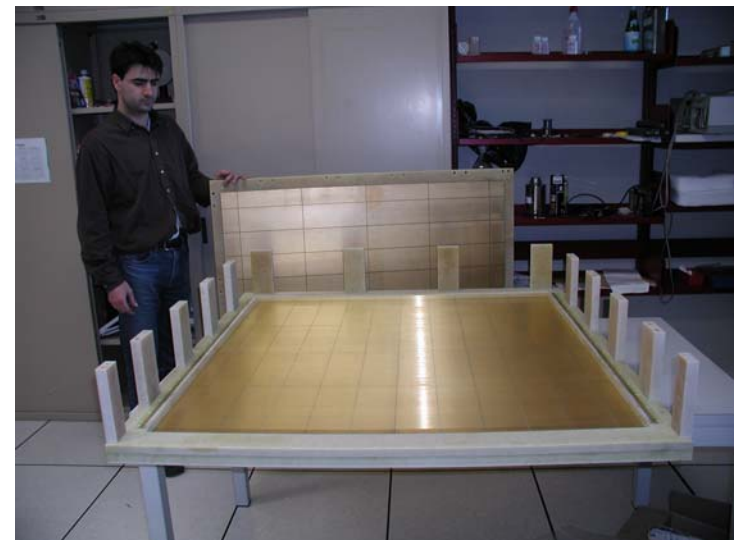
G.Montagnoli et al. LNL annual Report 2000 pg.165

10 sections Multiwire PPAC



S.Beghini et al. LNL annual Report 2000 pg.163

10 x 4 sections Ionization Chamber



Experiments performed: March-November 2004

- **Search for excited states in neutron rich ^{37}P and ^{39}P using deep inelastic processes. Medium spin –spectroscopy of Ne, Mg, and Si neutron rich isotopes** X.Liang, Paisley F.Azaiez, Orsay, Zs.Dombradi, Debrecen
 $(^{36}\text{S} + ^{208}\text{Pb})$
- **Nuclear spectroscopy of neutron rich nuclei in the N=50 region**
G.Duchene, Strasbourg, G.de Angelis, Legnaro
 $(^{82}\text{Se} + ^{238}\text{U})$
- **Spectroscopy of deformed neutron rich $A \sim 60$ nuclei**
S.M.Lenzi, Padova, S.J.Freeman, Manchester
 $(^{64}\text{Ni} + ^{238}\text{U})$
- **Pair transfer effects in $^{90}\text{Zr}+^{208}\text{Pb}$** L.Corradi, Legnaro
 $(^{90}\text{Zr} + ^{208}\text{Pb})$
- **Isotensor MED across the f7/2 shell: identification of the 6+ state in ^{54}Co**
A.Gadea, Legnaro
 $(^{54}\text{Fe} + ^{58}\text{Ni})$
- **Resonances in $^{24}\text{Mg}+^{24}\text{Mg}$ and molecular states in ^{48}Cr**
F.Haas, Strasbourg
 $(^{24}\text{Mg} + ^{24}\text{Mg})$
- **Anomalous MED in ^{31}S .** D.R.Napoli, M.Marginean, Legnaro
 $(^{32}\text{S} + ^{58}\text{Ni})$

$^{82}\text{Se} + ^{238}\text{U}$ E=505 MeV (ALPI)

4 days, PRISMA at $\theta_G=64^\circ$

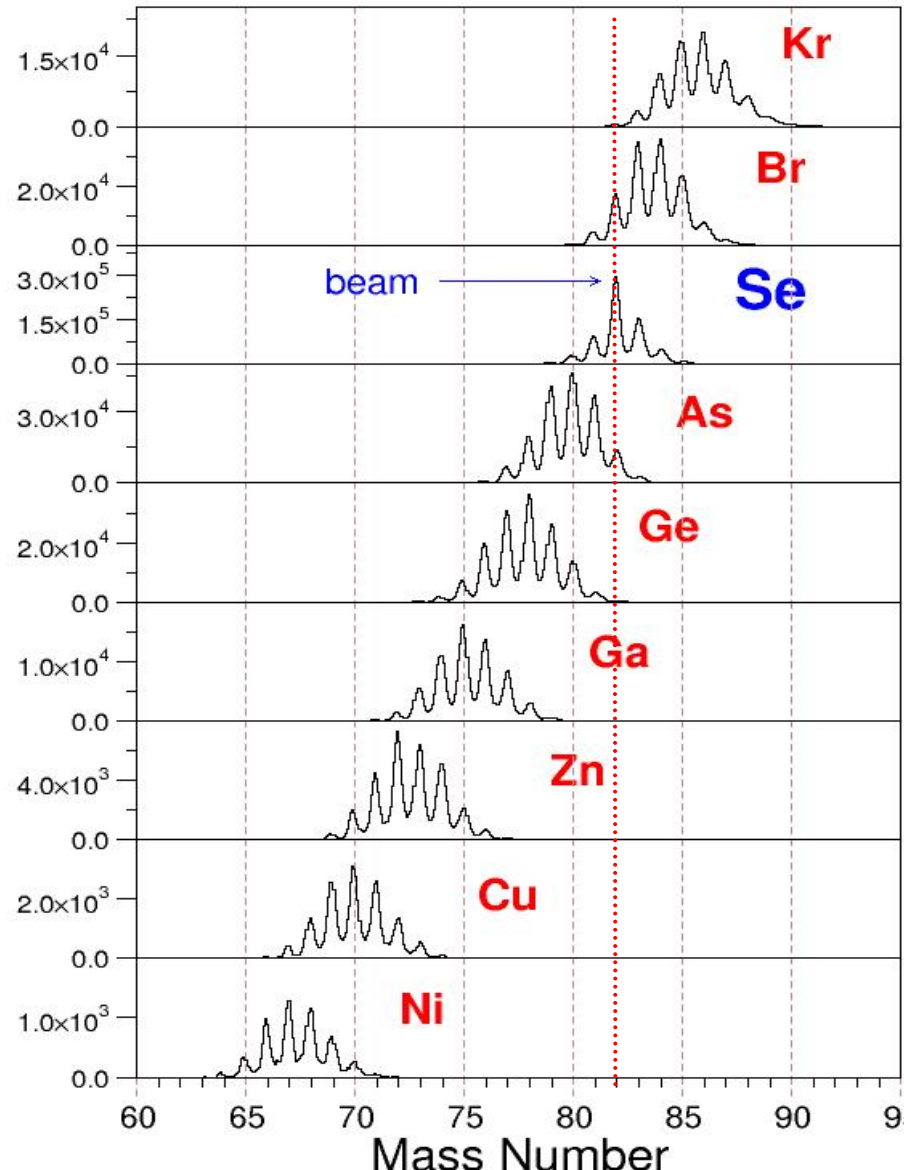
G.deAngelis, G.Duchêne
Analysis: N.Marginean

Kr76 14.8 h 0+	Kr77 74.4 m 5/2+	Kr78 0+	Kr79 35.04 h 1/2-	Kr80 2.29E+5 y 7/2+	Kr81 0+	Kr82 11.6	Kr83 9/2+	Kr84 0+	Kr85 10.756 y 9/2+	Kr86 0+	Kr87 76.3 m 5/2+	Kr88 2.84 h 0+	
Br75 96.7 m 3/2-	Br76 16.2 h 1- *	Br77 57.036 h 3/2- *	Br78 6.46 m 1+	Br79 2.25 3/2- *	Br79 50.69	Br80 17.68 m 1+	Br81 3/2-	Br82 35.30 h 5-	Br83 2.40 h 3/2-	Br84 31.80 m 0+	Br85 2.90 m 3/2-	Br86 55.1 s (2-)	Br87 55.60 s 3/2-
Se74 0+	Se75 119.779 d 5/2+	Se76 0+	Se77 0+	Se78 9.36	Se79 7.63	Se80 49.61	Se81 1.13E6 y 7/2+	Se82 1.08E+20 y 0+	Se83 22.3 m 9/2+	Se84 3.1 m 0+	Se85 31.7 s (5/2+)	Se86 15.3 s 0+	
As73 80.30 d 3/2-	As74 17.77 d 2-	As75 100 3/2-	As76 1.0778 d 2-	As77 38.83 h 3/2-	As78 90.7 m 2-	As79 9.01 m 3/2-	As80 15.5 s 1+	As81 1.0 s 0+	As82 19.1 s (1+)	As83 13.4 s (5/2-,3/2-)	As84 4.02 s	As85 2.021 s (3/2-)	
Ge72 0+	Ge73 9/2+	Ge74 0+	Ge75 82.78 m 1/2-	Ge76 0+	Ge77 11.30 h 7/2+	Ge78 85.0 m 0+	Ge79 18.98 s (1/2-)	Ge80 1.0 s 0+	Ge81 1.0 s 0+	Ge82 4.60 s 0+	Ge83 1.85 s (5/2+)	Ge84 966 ms 0+	
Ga71 3/2- 39.892	Ga72 14.10 h 3-	Ga73 4.86 h 3/2-	Ga74 8.12 m (3-)	Ga75 126 s 3/2-	Ga76 32.6 s (2+,3+)	Ga77 13.2 s (3/2-)	Ga78 5.09 s (3+)	Ga79 2.847 s (3/2-)	Ga80 1.697 s (3)	Ga81 1.217 s (5/2-)	Ga82 0.599 s (1,2,3)	Ga83 0.31 s	
Zn70 5E:14 y 0.6	Zn71 2.45 m 1/2-	Zn72 46.5 h 0+	Zn73 23.5 s (1/2-)	Zn74 95.6 s 0+	Zn75 102 s (7/2+)	Zn76 5.7 s 0+	Zn77 2.08 s (7/2+)	Zn78 1.47 s 0+	Zn79 995 ms (9/2+)	Zn80 0.545 s 0+	Zn81 0.29 s	Zn82 0+	
Cu69 2.85 m 3/2-	Cu70 4.5 s (1+)	Cu71 19.5 s (3/2-)	Cu72 6.6 s (1+)	Cu73 3.9 s	Cu74 1.594 s (1+,3+)	Cu75 1.224 s	Cu76 0.641 s	Cu77 469 ms	Cu78 342 ms	Cu79 188 ms	Cu80	52	
Ni68 19 s 0+	Ni69 11 s 0+	Ni70 0+	Ni71 1.86 s	Ni72 2.1 s 0+	Ni73 0.90 s	Ni74 1.1 s 0+	Ni75	Ni76 0+	Ni77	Ni78 0+			

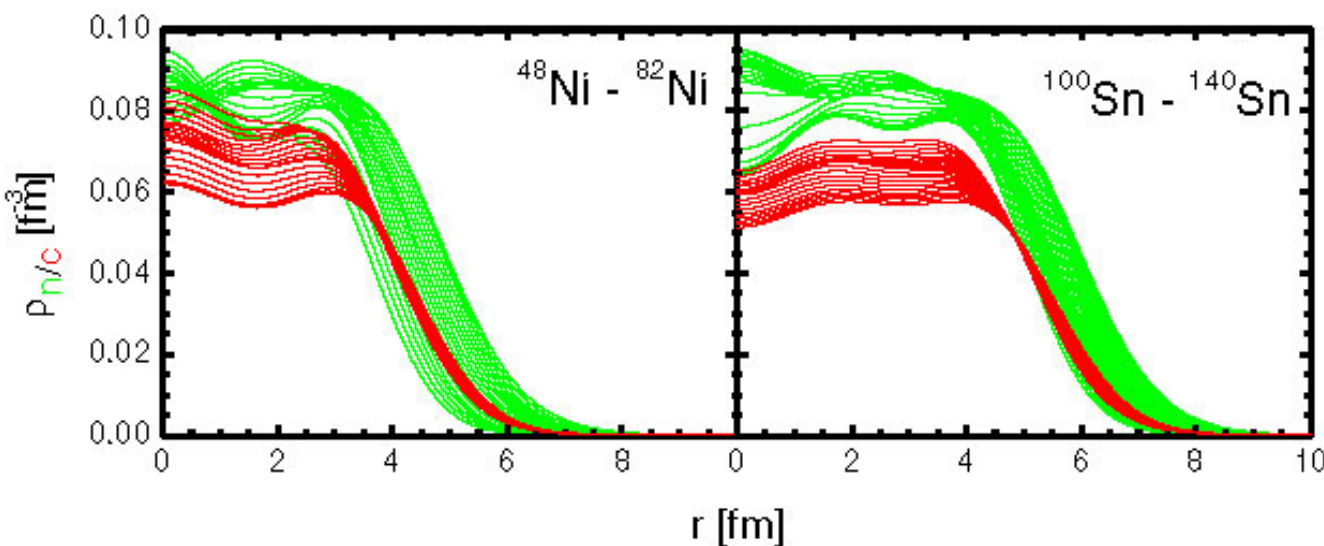
40 42 44 46 48 50

50

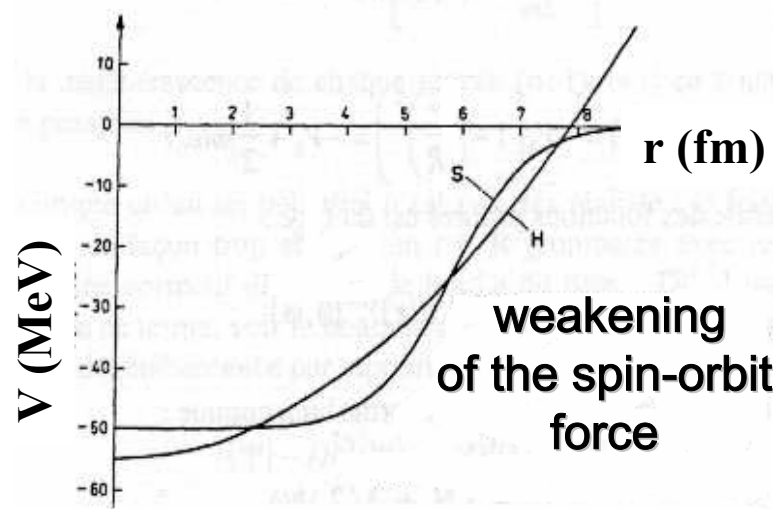
Evolution of the N=50 shell: Searching
for the shell gap quenching
(onset of deformation as in N=20 Z~12)



Z=32: INM, R.C.Nayak et al.
PRC 60 (1999) 064305
Z=24-26: RMF, L.S.Geng et al.
nucl-th/0402083



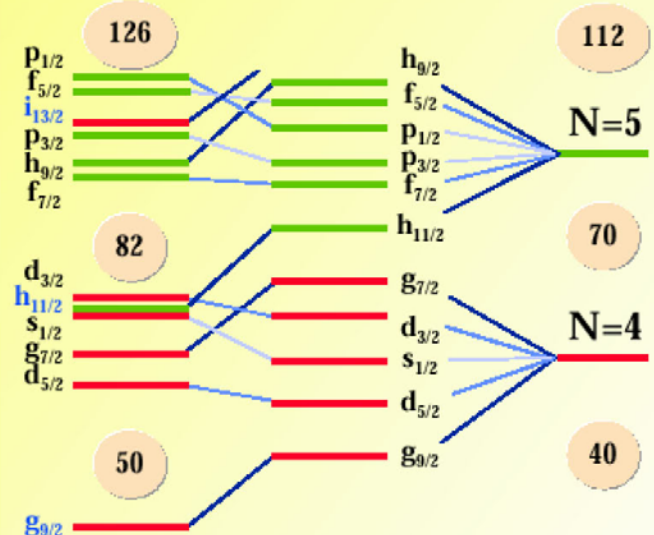
F.Hofmann, C.M.Keil, H.Lenske, Phys.Rev.C64(01)034314.



G.A.Lalazissis, D.Vretenar, P.Ring, Phys.Rev.C57(98)2294.
D.Vretenar, G.A.Lalazissis, P.Ring, Phys.Rev.C57(98)3071.
J.Meng, I.Tanihata, Nucl.Phys.A650(99)176.

Change of the shell structure in neutron-rich nuclei close to the drip-line

Nuclear Shell Structure

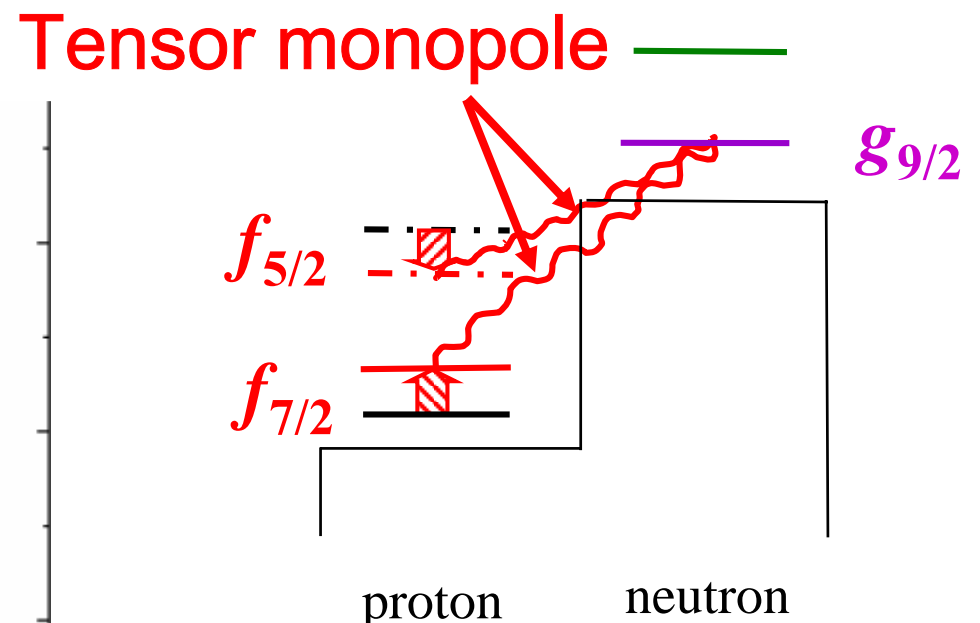
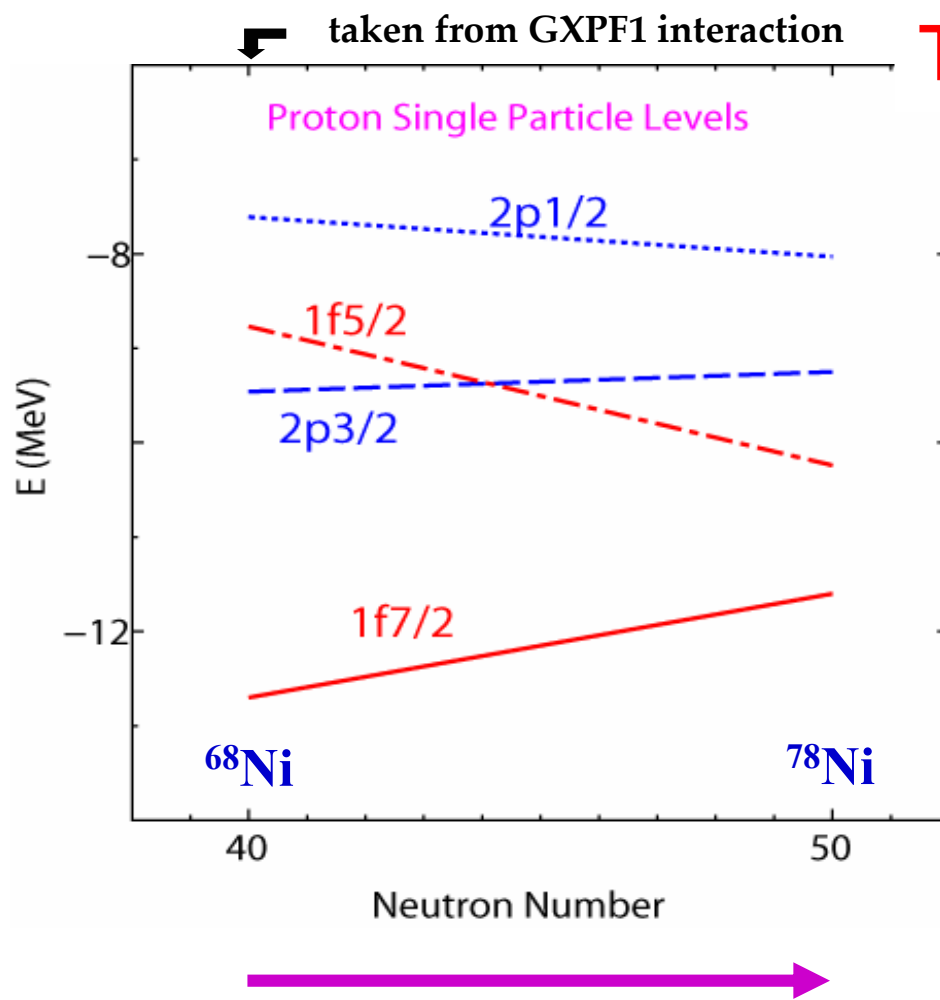


around
the
valley of
B-STABILITY

very diffuse
surface
neutron drip line

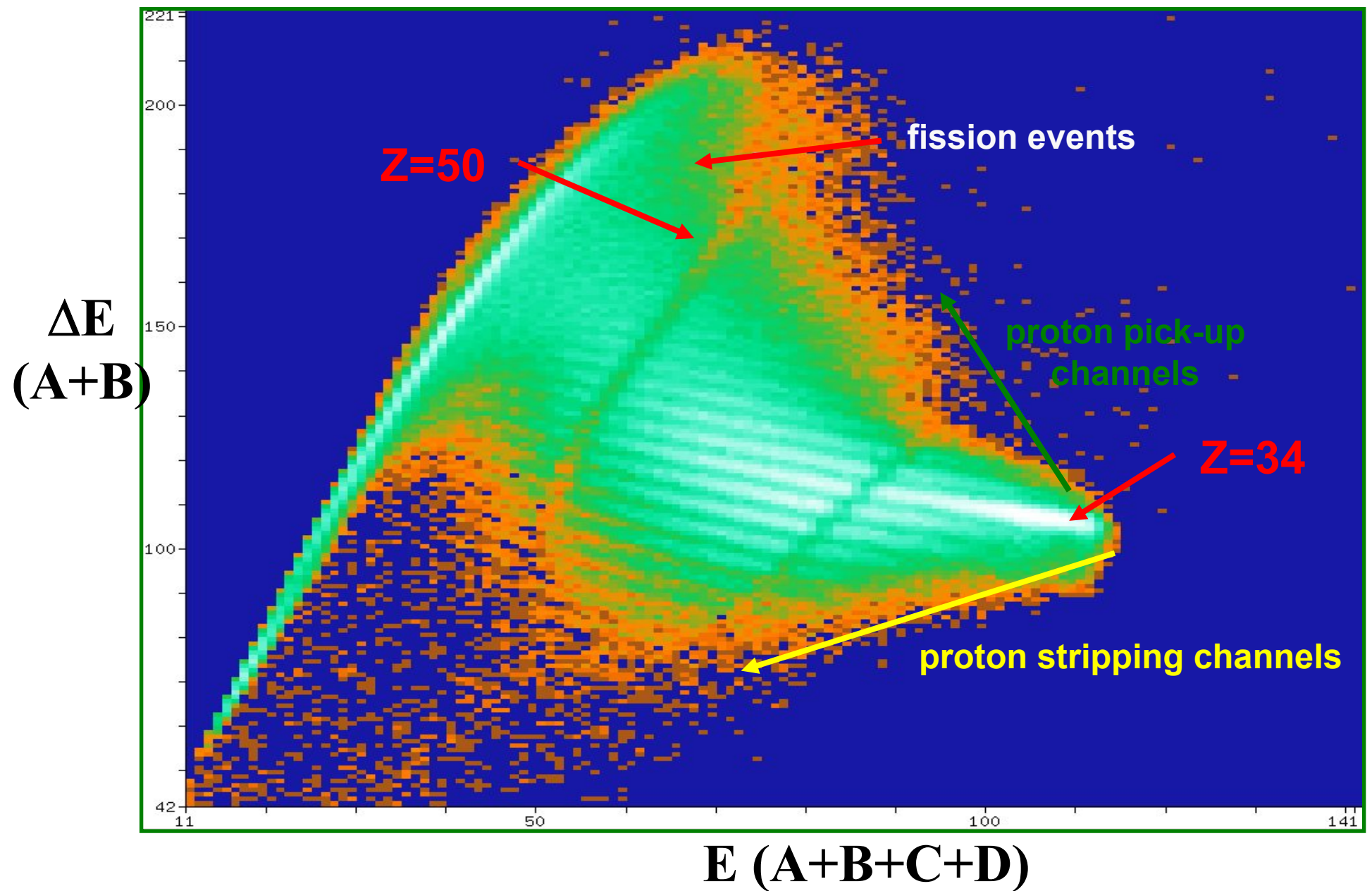
harmonic
oscillator

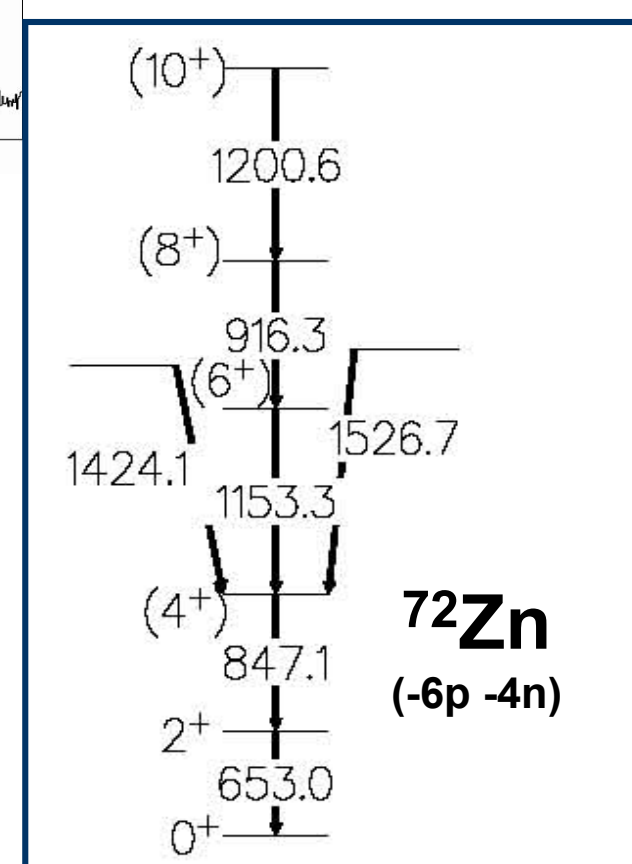
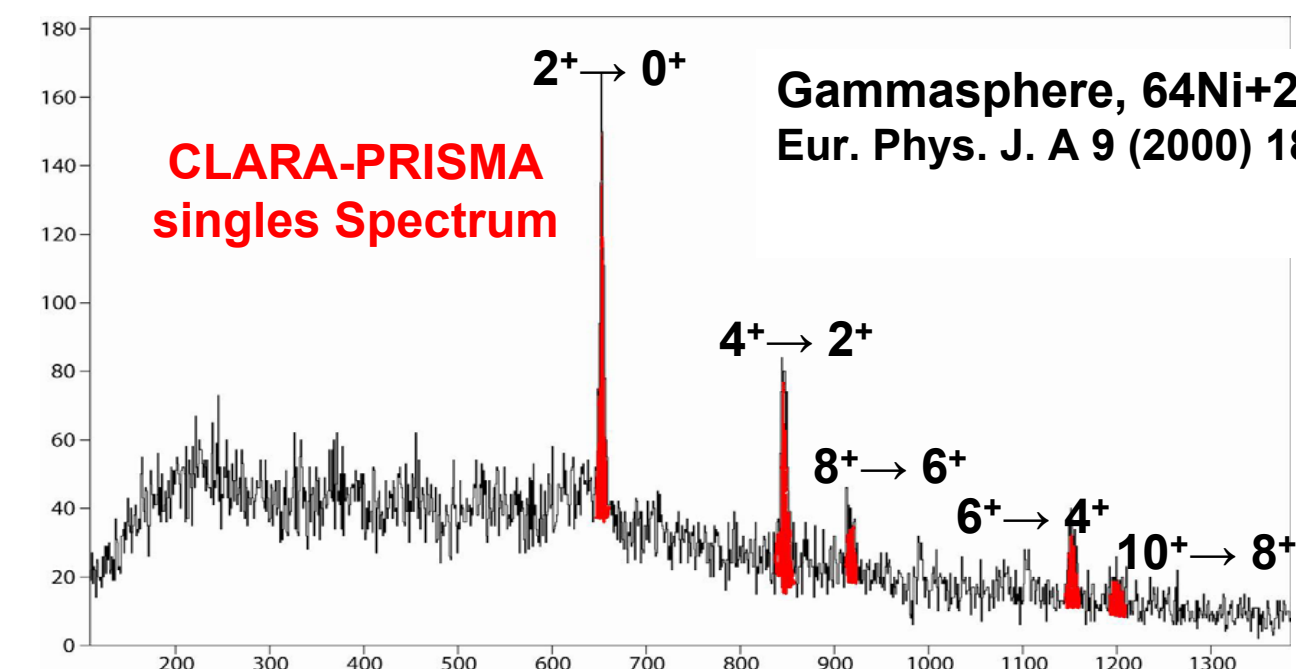
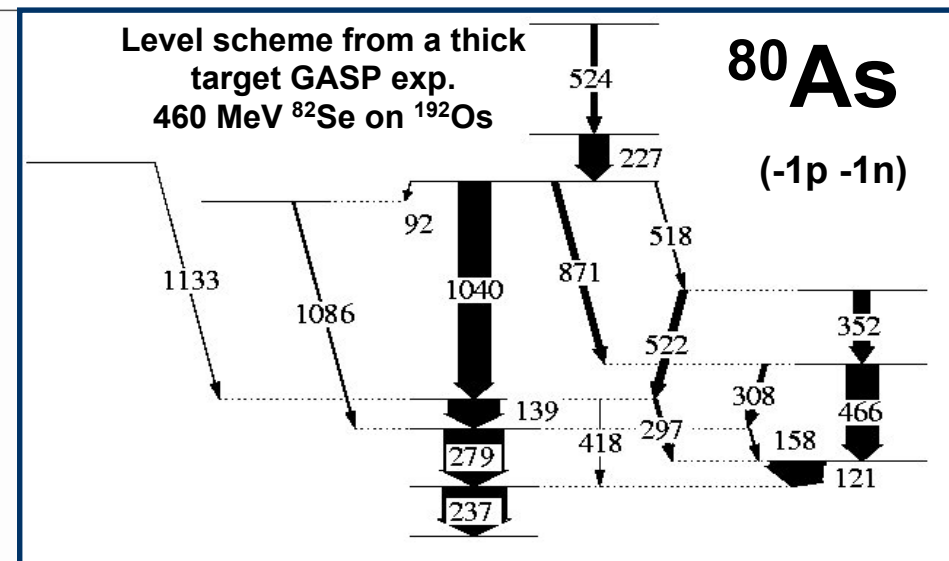
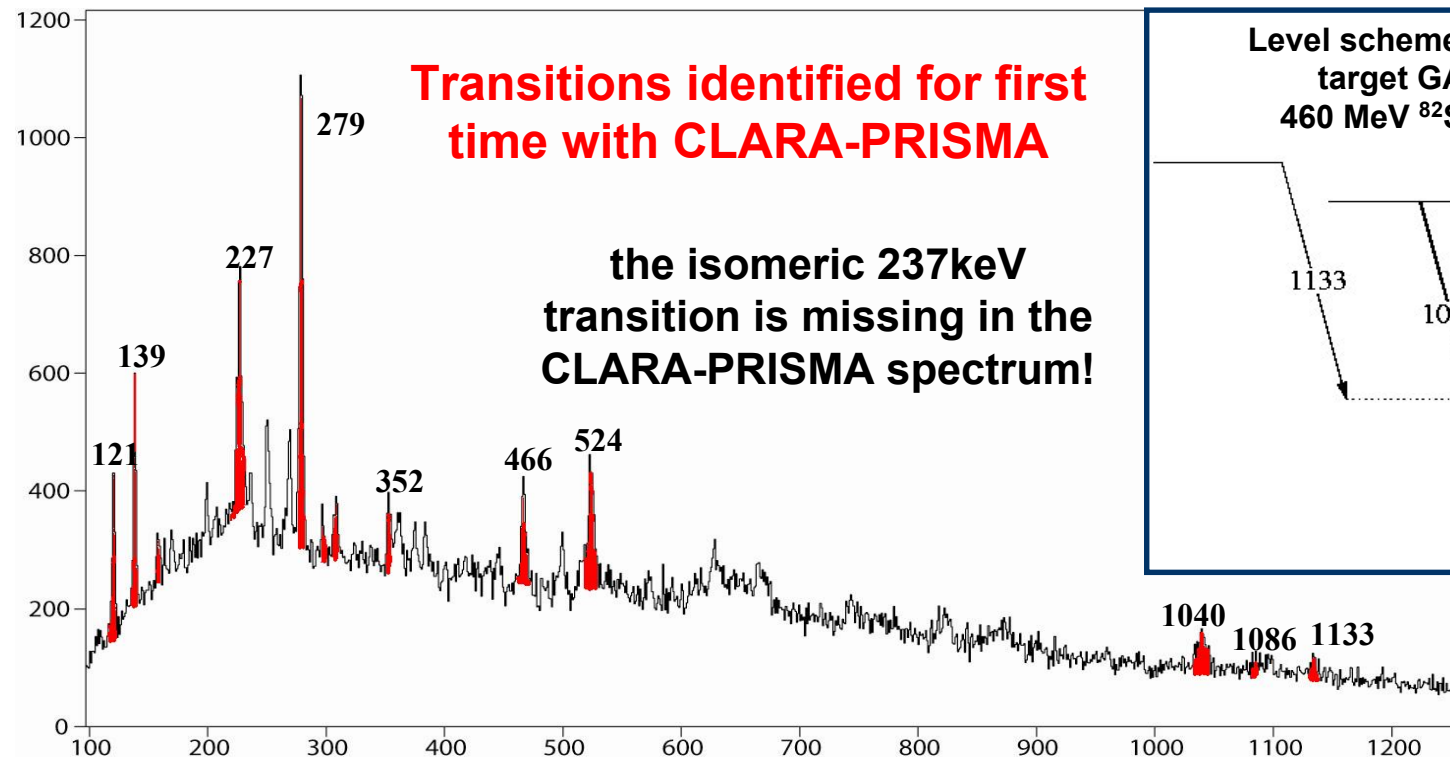
Drip line effects are not the only cause of shell evolution.
 Tensor interaction ($\pi + \rho$ meson) may be responsible for the
 weakening of the N=50 gap



Low-lying 2^+ levels in Ni,
 M. Sawicka et al.,
 Phys. Rev. C68 (03) 044304

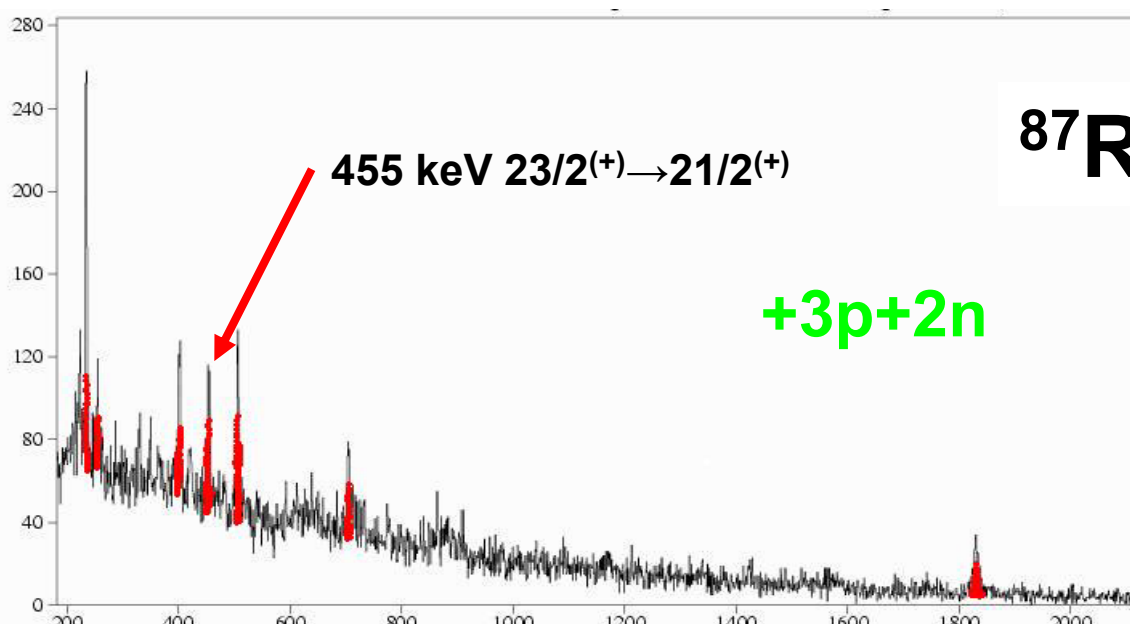
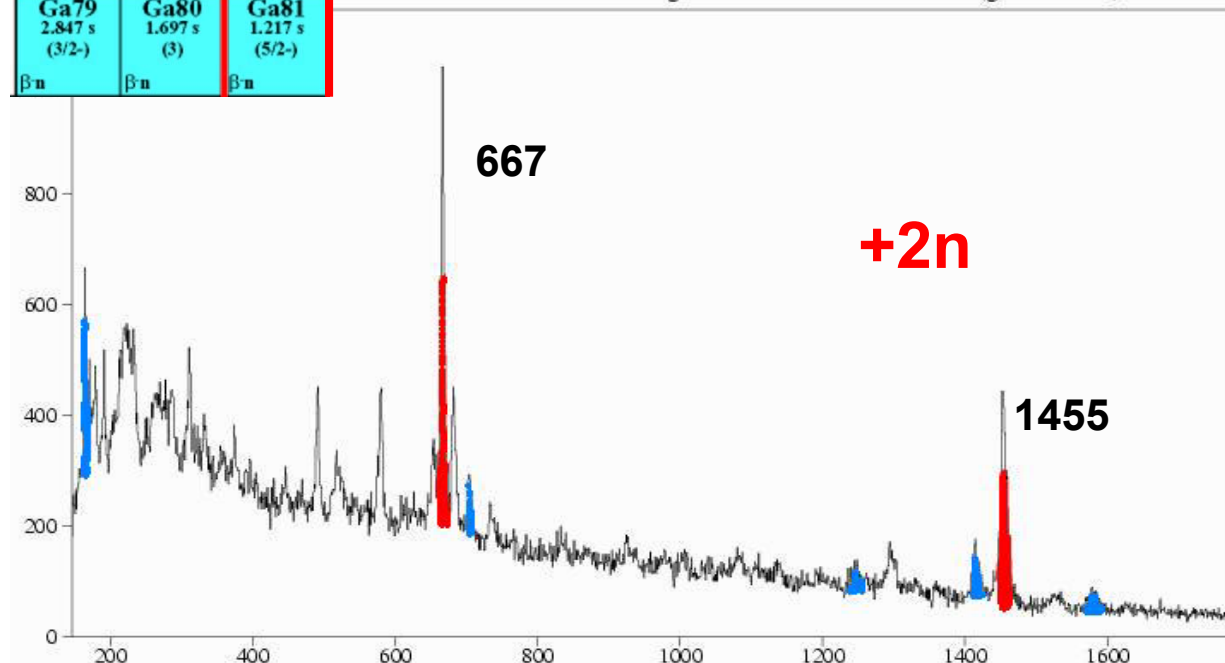
$^{82}\text{Se} + ^{238}\text{U}$ E=505 MeV $\theta_G=64^\circ$ IC ΔE -E Matrix



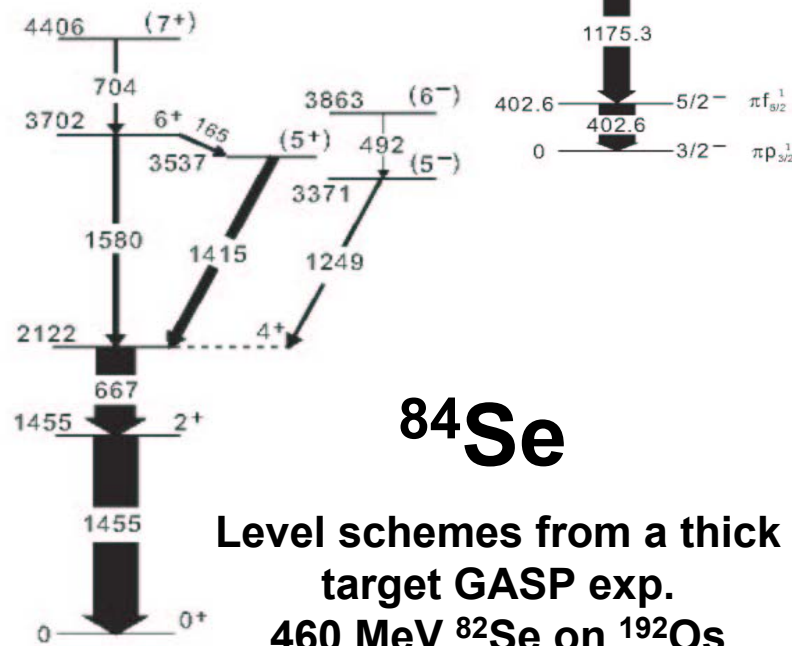
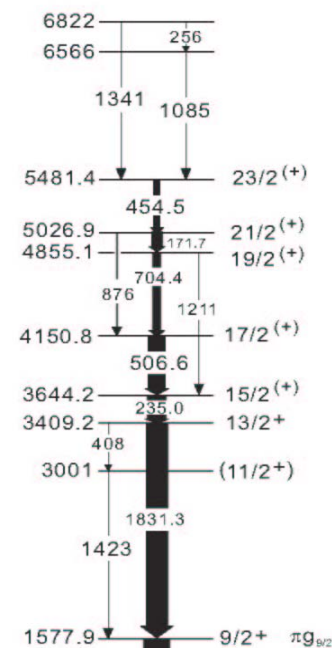


$^{82}\text{Se} + ^{238}\text{U}$ E=505 MeV

Sr86	Sr87	Sr88
0+	9/2+ *	0+
9.86	7.00	82.58
Rb85	Rb86 18.631 d	Rb87 4.75E10 y
5/2-	-	5/2-
Kr84	EC, β^-	β^-
Kr85 10.756 y	9/2+	0+
0		17.3
57	β^-	
Br83 2.4 s	Br84 31.80 m	Br85 2.90 m
3/2-	2-	3/2-
β^-	β^-	β^-
Se82 1.08E+20 y	Se83 22.3 m	Se84 3.1 m
0+	*	0+
$\beta\beta^-$	β^-	β^-
3.73		
As81 33.3 s	As82 19.1 s	As83 13.4 s
3/2-	(1+)	(5/2-, 3/2-)
β^-	β^-	β^-
Ge80 29.5 s	Ge81 7.6 s	Ge82 4.60 s
0+	(9/2+)	0+
β^-	β^-	β^-
Ga79 2.847 s	Ga80 1.697 s	Ga81 1.217 s
(3/2-)	(3)	(5/2-)
β^- n	β^- n	β^- n



87Rb

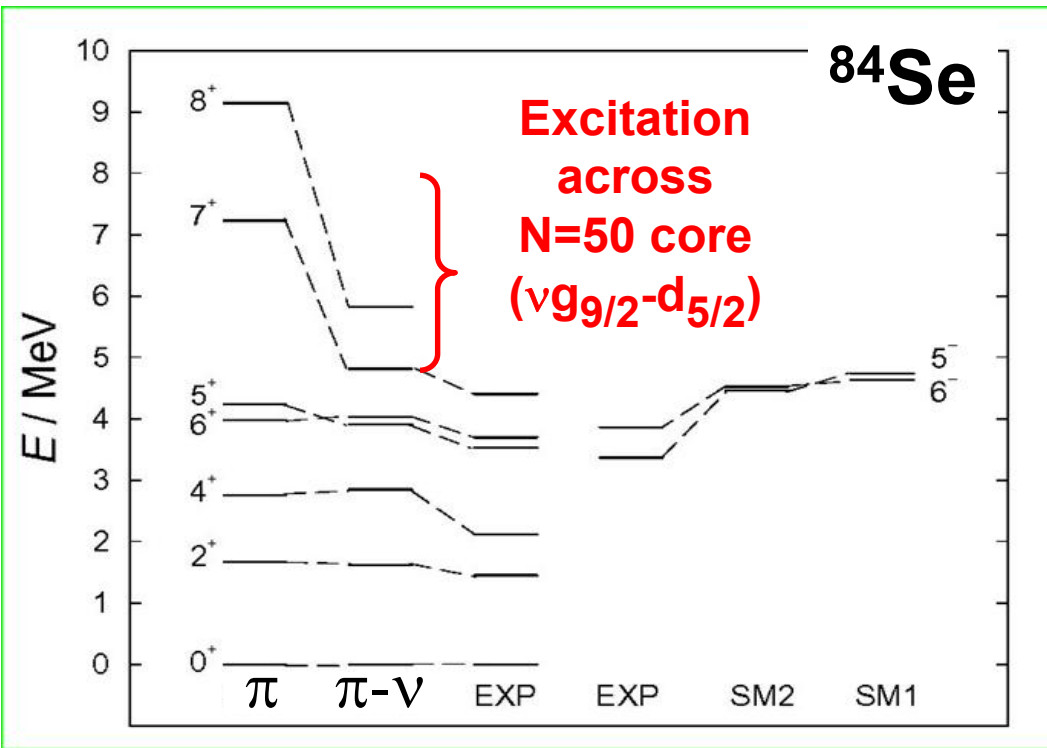


84Se

Level schemes from a thick target GASP exp.
460 MeV ^{82}Se on ^{192}Os

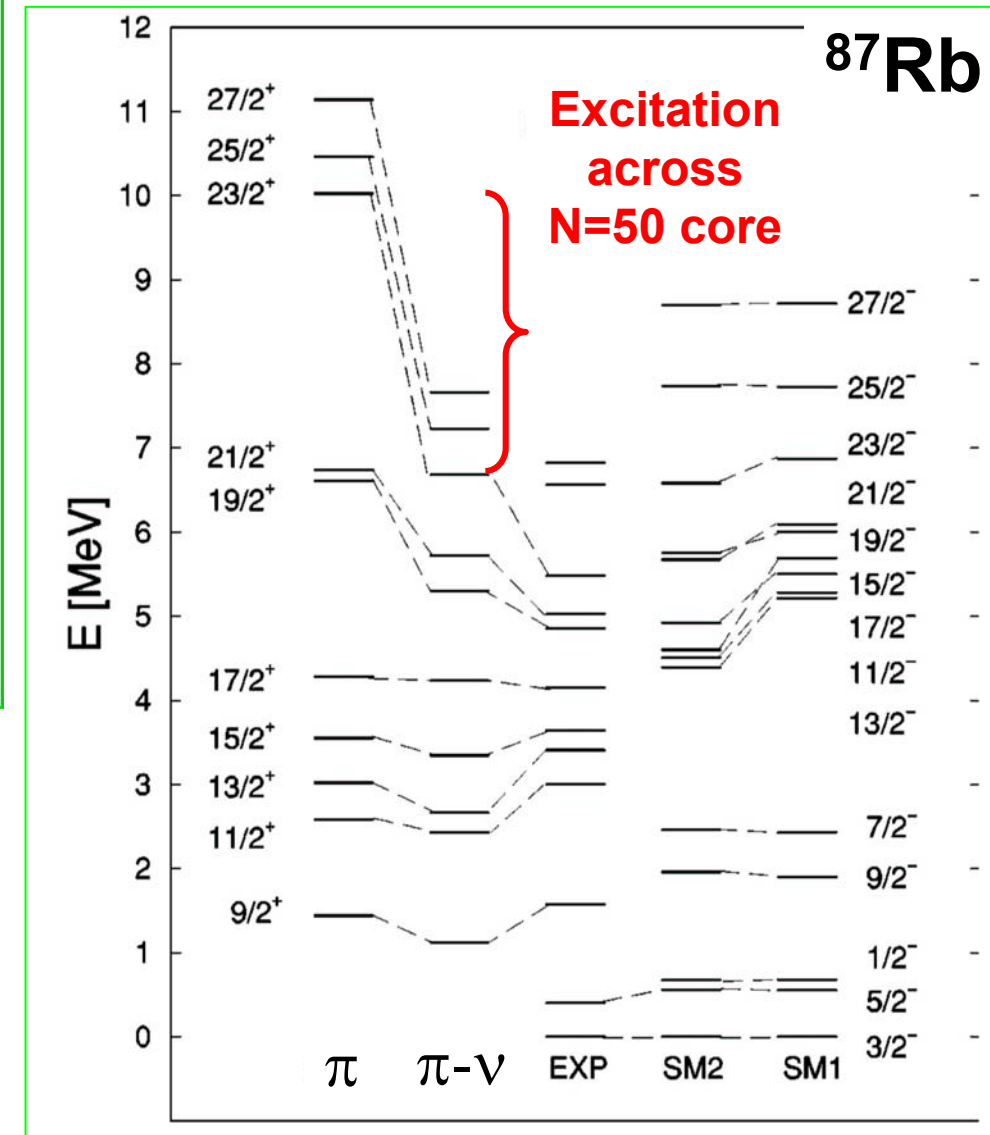
Stability of the N=50 Shell down to Z~32

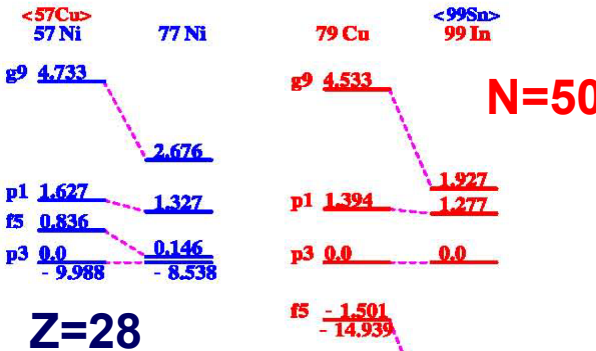
Shell model with renormalized SPE ($f_{5/2}$ - $g_{9/2}$)
 TBME: X.Ji & B.H. Wildenthal PRC 37(1988)1256
 SPE: Lisetskiy et al., nucl-th/0402082



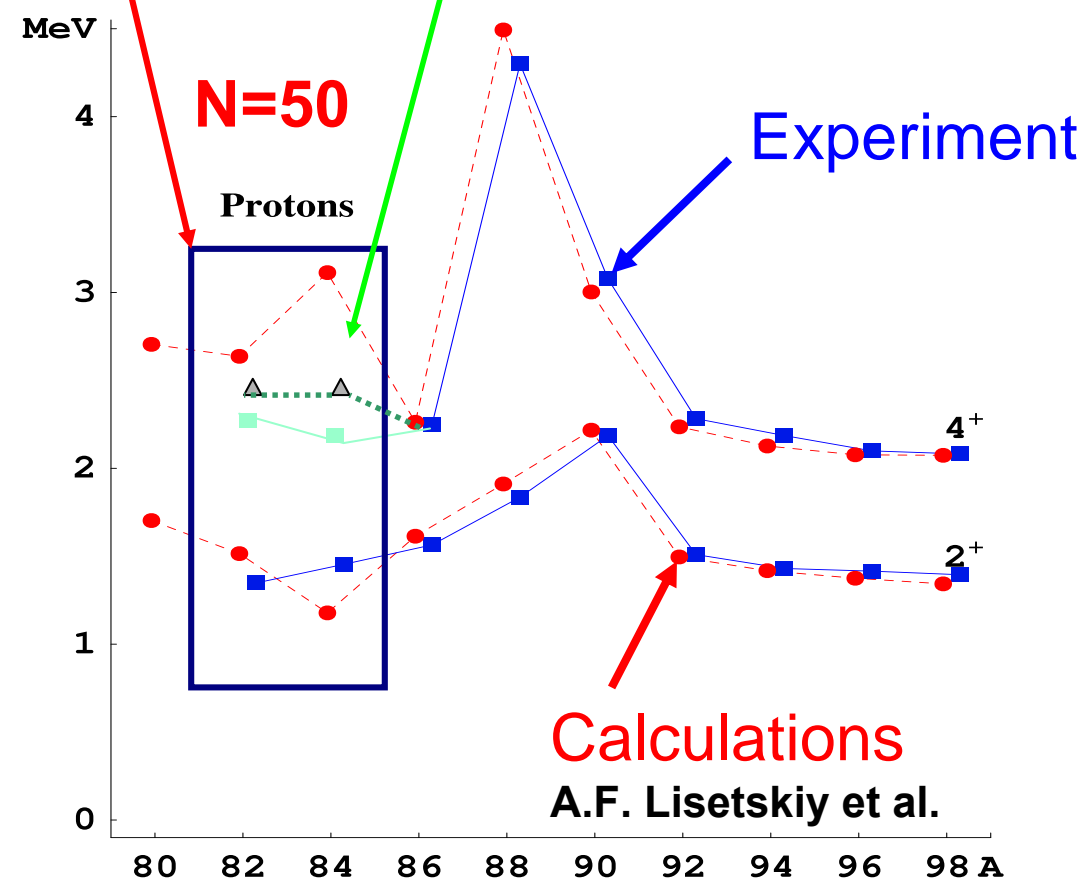
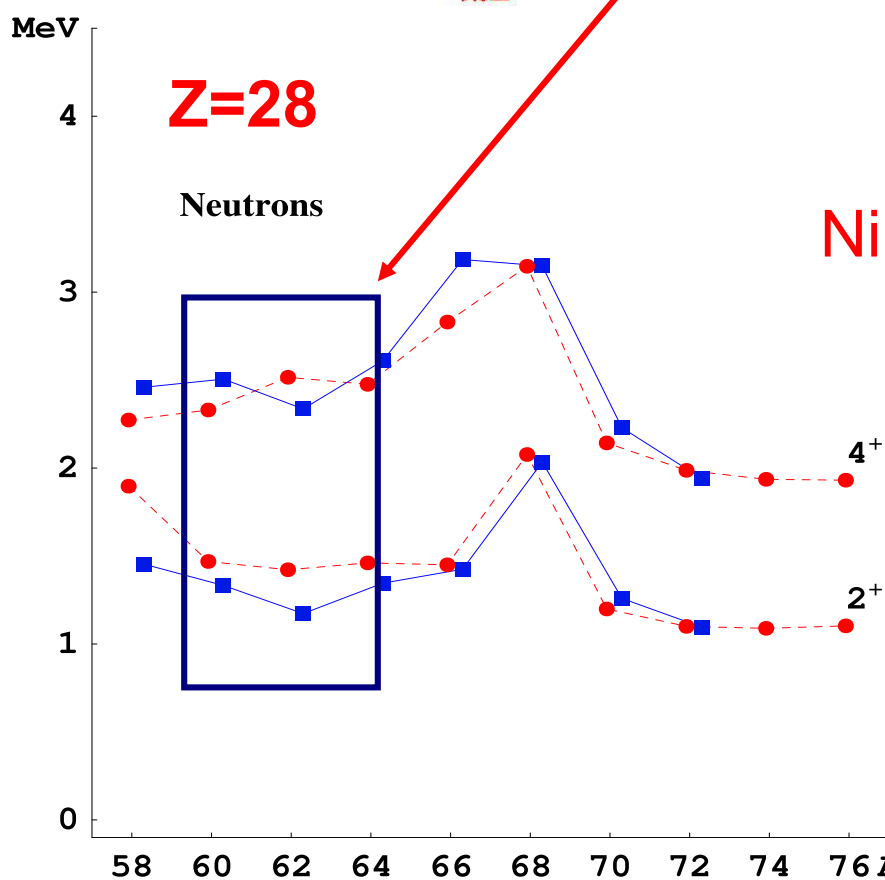
Space: $\pi f_{5/2} p_{3/2} p_{1/2} g_{9/2} \nu p_{1/2} g_{9/2} d_{5/2}$

The description of these semi-magic nuclei (within the shell model framework) can be done with a constant **N=50** shell gap.





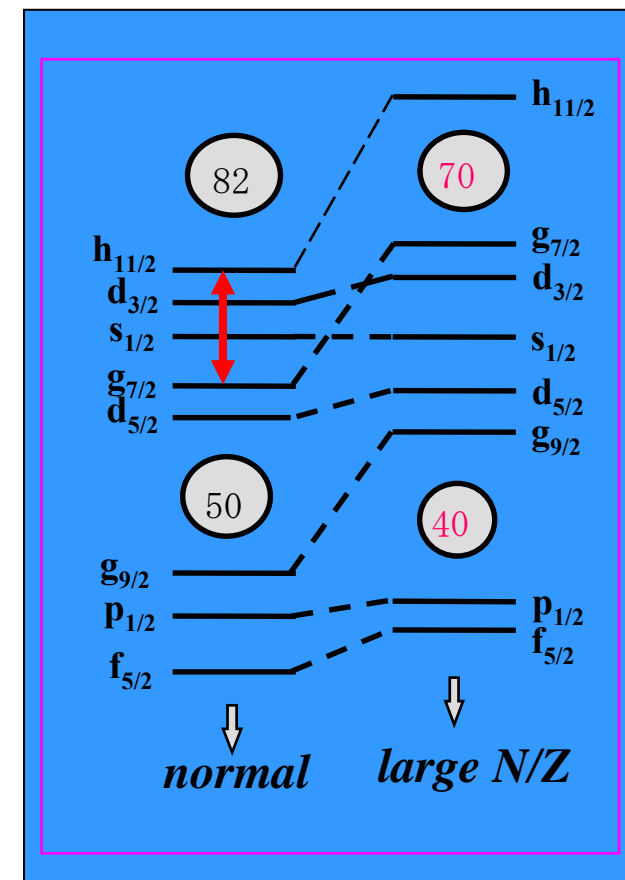
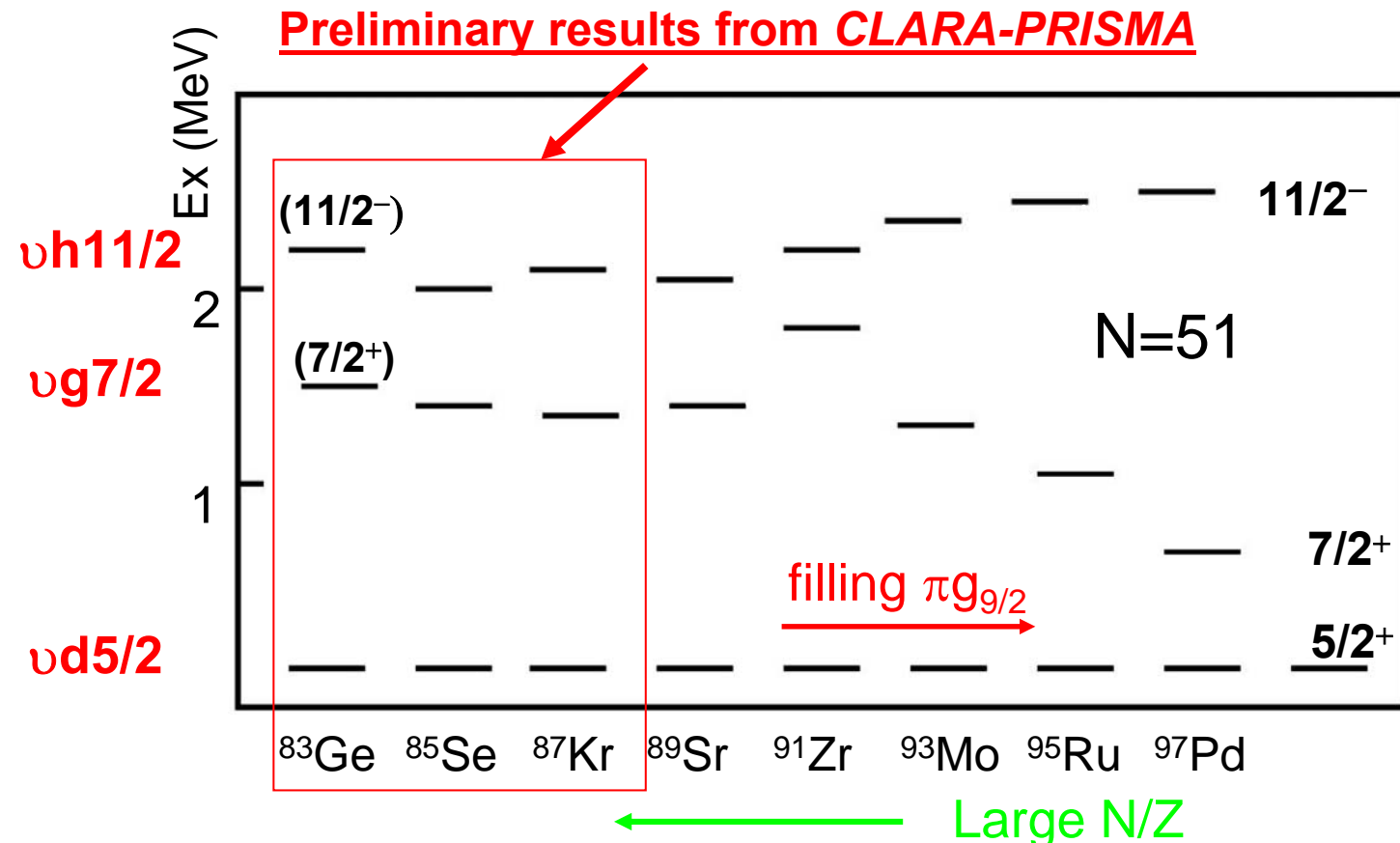
Valence Mirror Symmetry restored



$N=51$
isotones

Monopole shift of the single particle levels ?

Downward shift of the $\nu g_{7/2}$ in proton rich $N=51$ isotones as $\pi g_{9/2}$ is filled
 The $\nu d_{5/2}$ - $h_{11/2}$ splitting is “constant” in neutron rich $N=51$ isotones: it should increase if the l_s term was getting weaker – No diffused potential?

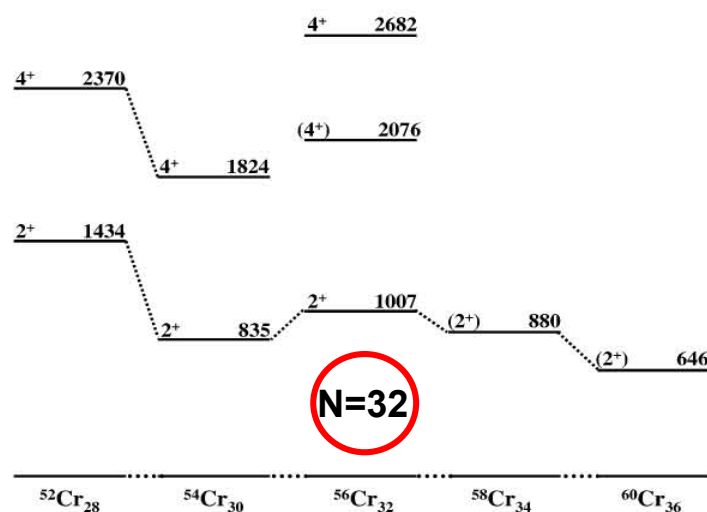
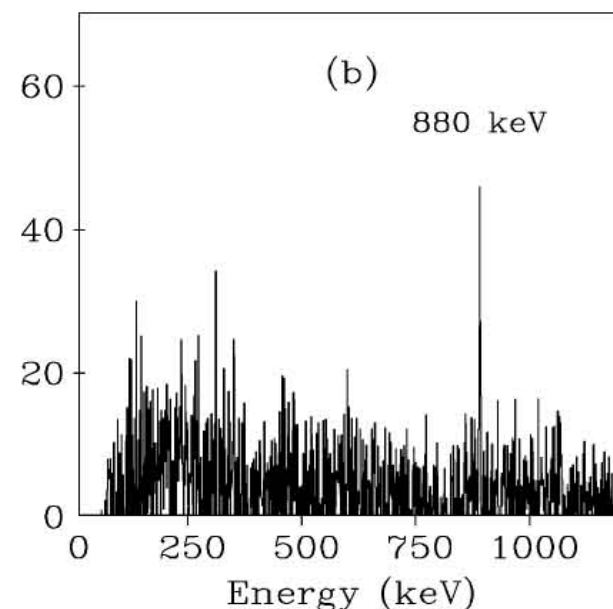
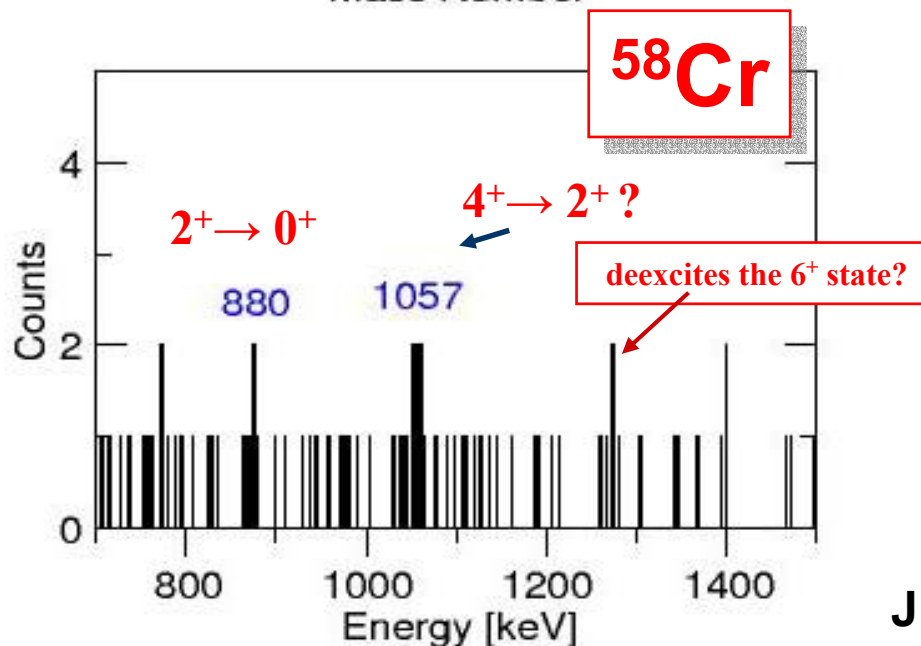
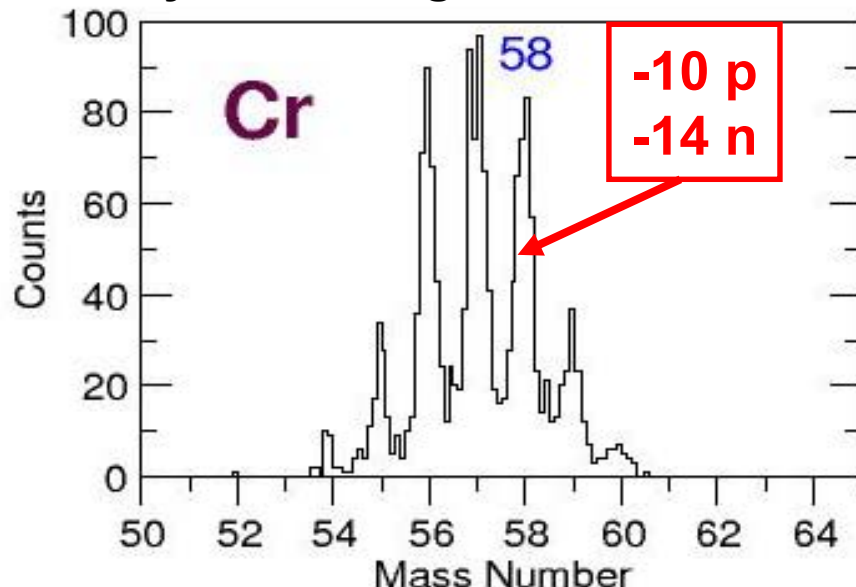


^{82}Se 505 MeV + ^{238}U

24 nucleons removed from projectile

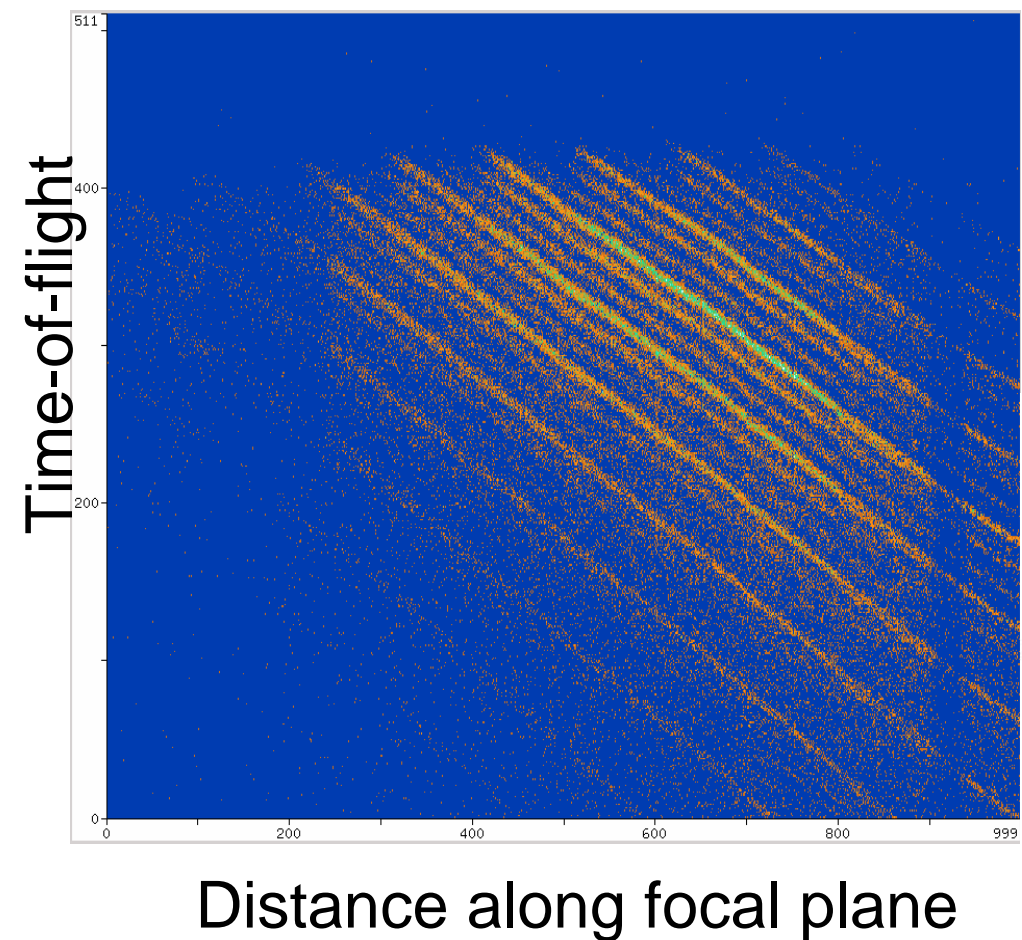
G.deAngelis, G.Duchêne

Analysis: N.Marginean

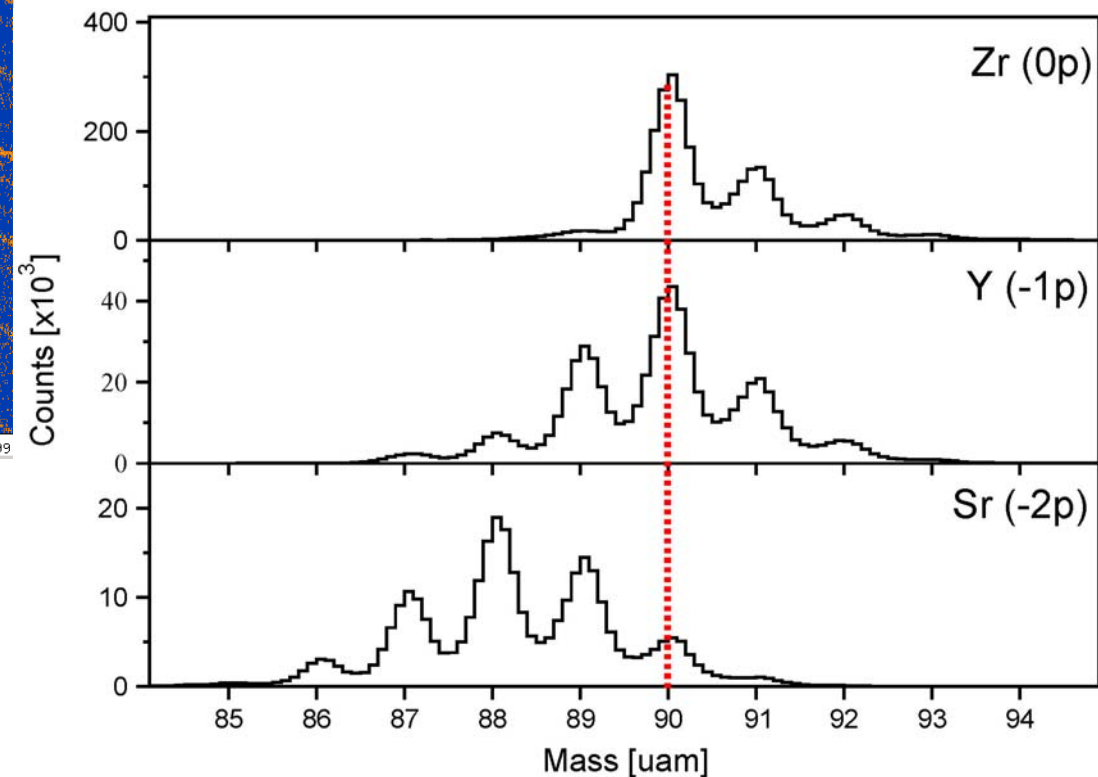


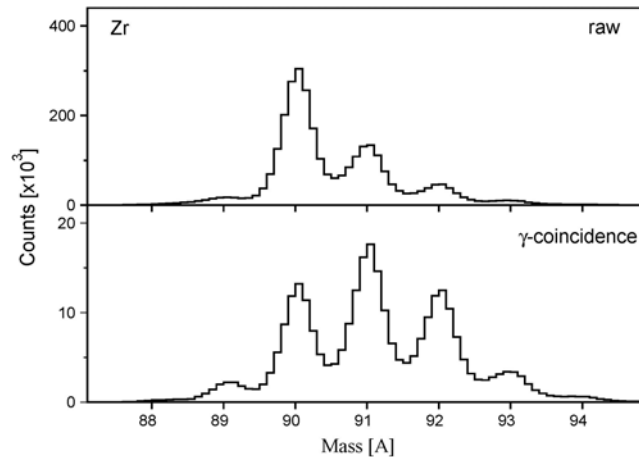
^{90}Zr 560MeV + ^{208}Pb

1 day beam time (4 pnA)
L.Corradi, C.A.Ur, et al.



Nb^{89} 1.9h (92+)	Nb^{90} 14.0h 8+	Nb^{91} 2.0h 92+	Nb^{92} 34.0h 7+	Nb^{93} 2.8h	Nb^{94} 20.0h 6+	Nb^{95} 34.9h 4+
HC	HC	HC	HC	100	0	0
Ir^{88} 23.4h 0+	Ir^{89} 72.4 h 92+	Ir^{90} 0+	Ir^{91} 52+	Ir^{92} 0+	Ir^{93} 1.53h 52+	Ir^{94} 0+
HC	HC	5.46	11.22	17.15	0	17.38
Y^{87} 70.8h 1/2	Y^{88} 103.6h 4	Y^{89} 12-	Y^{90} 64.0h 2-	Y^{91} 52.1h 1/2	Y^{92} 35.4h 2-	Y^{93} 101.8h 1/2
HC	HC	1.0	0	0	0	0
Sr^{86} 0+	Sr^{87} 92+	Sr^{88} 0+	Sr^{89} 50.5h 52+	Sr^{90} 22.2h 0+	Sr^{91} 9.6h 52+	Sr^{92} 2.3 h 0+
92+	7.00	52+	0	0	0	0
Rb^{85} 52+	Rb^{86} 18.0h 2-	Rb^{87} 47.9h 2-	Rb^{88} 17.7h 2-	Rb^{89} 15.1h 3/2	Rb^{90} 1.9h 0	Rb^{91} 55.4h 3/2-)
72.05	HC, 0	0	0	0	0	0





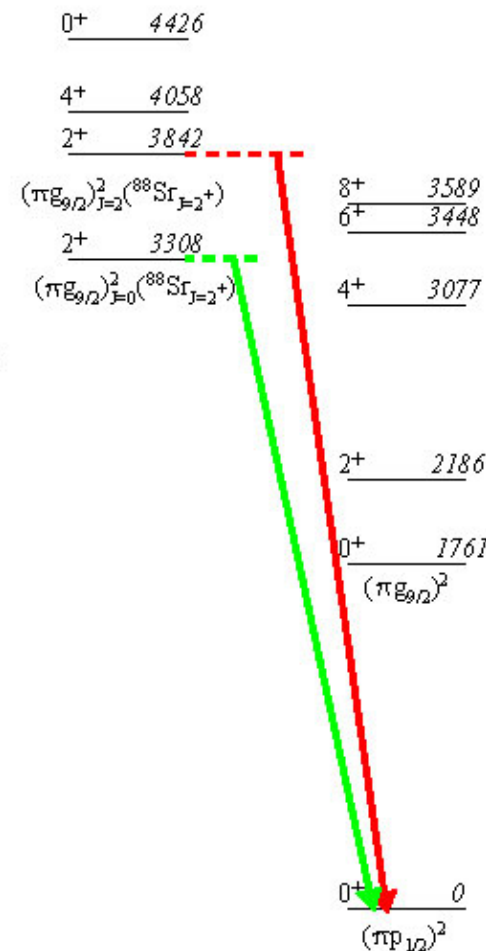
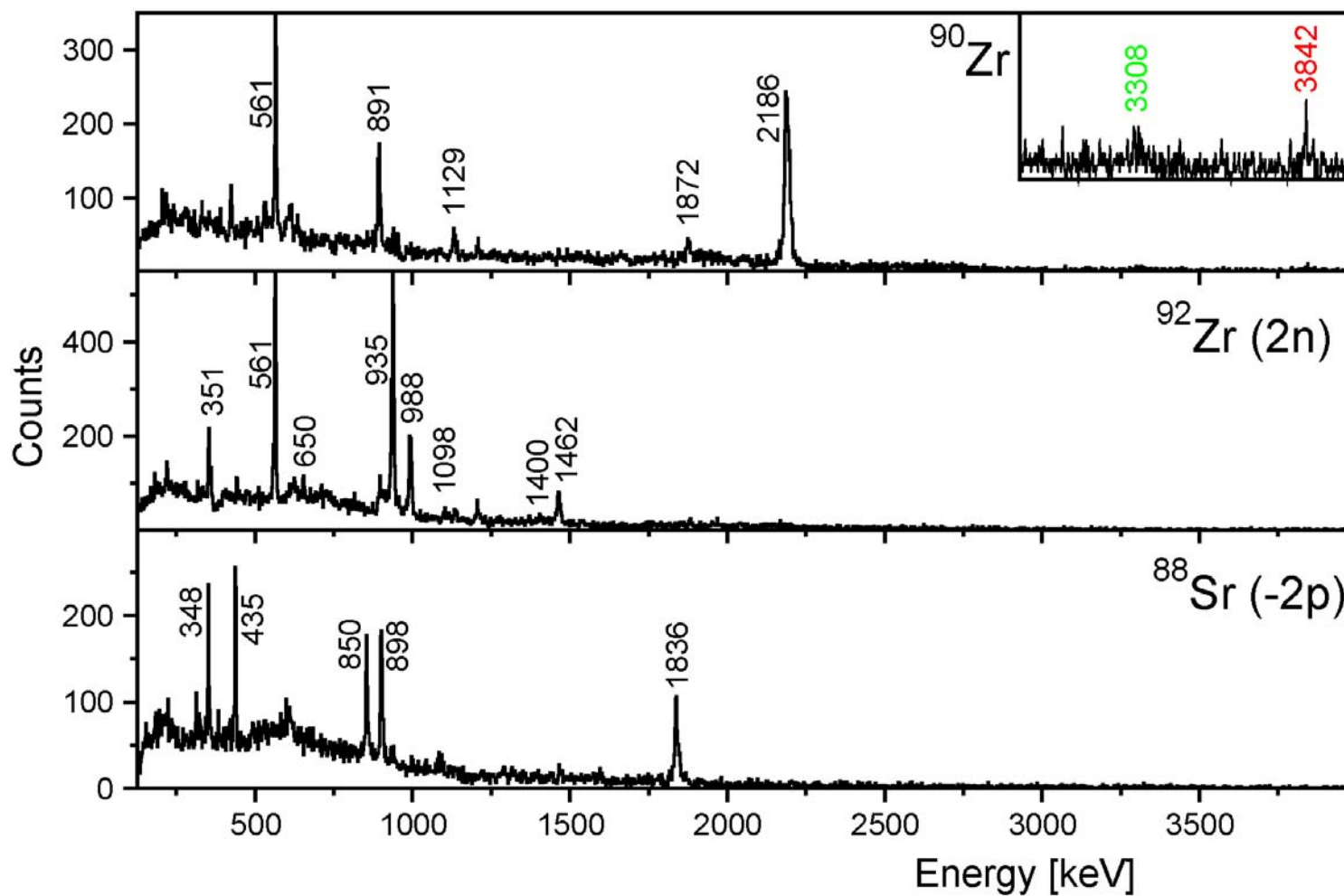
**^{90}Zr 560MeV
+ ^{208}Pb**

L.Corradi, C.A.Ur et al.

0^+ 4124
 2^+ 3842

2-phonon pairing vib.

3^- 2748
oct.phonon



Spectroscopy of deformed neutron rich A ~ 60 nuclei

Ni56 6.077 d 0+	Ni57 35.60 h 3/2-	Ni58 0+ EC	Ni59 7.6E+4 y 3/2- EC	Ni60 0+ EC	Ni61 3/2- EC	Ni62 0+ EC	Ni63 100.1 y 1/2- β^-	Ni64 0+ 0.926 β^-	Ni65 2.5172 h 5/2- β^-
Co55 17.53 h 7/2- EC	Co56 77.27 d 4+ EC	Co57 271.79 d 7/2- EC	Co58 70.82 d 2+ *	Co59 7/2- 100	Co60 5.2714 y 5+ *	Co61 1.650 h 7/2- β^-	Co62 1.50 m 2+ *	Co63 1.4 s 2+ β^-	Co64 0.30 s 1+ β^-
Fe54 0+ 5.8 EC	Fe55 2.73 y 3/2- EC	Fe56 0+ 91.72	Fe57 1/2- 2.2	Fe58 0+ 0.28	Fe59 44.503 d 3/2- β^-	Fe60 1.5E+6 y 0+ β^-	Fe61 5.98 m 3/2-, 5/2- β^-	Fe62 1.62 s 1/2- β^-	Fe63 6.1 s (5/2-) β^-
Mn53 3.74E+6 y 7/2- EC	Mn54 312.3 d 3+ EC, β^-	Mn55 5/2- 100	Mn56 2.5785 h 3+ β^-	Mn57 85.4 s 5/2- β^-	Mn58 3.0 s 0+ *	Mn59 4.6 s 0+ *	Mn60 51 s 3/2-, 5/2- 0+ *	Mn61 1 s 0+ *	Mn62 0.88 s (3+) β^-
Cr52 0+ 83.789	Cr53 3/2- 9.501	Cr54 0+ 2.365	Cr55 3.497 m 3/2- β^-	Cr56 5.94 m 0+ β^-	Cr57 21.1 s 3/2-, 5/2-, 7/2- β^-	Cr58 7.0 s 0+ β^-	Cr59 0.4 s 0+ β^-	Cr60 0.7 s 0+ β^-	Cr61 β^-
V51 7/2- 99.750	V52 3.743 m 3+ β^-	V53 1.61 m 7/2- β^-	V54 49.8 s 3+ β^-	V55 6.54 s (7/2-) β^-	V56 β^-	V57 β^-	V58 β^-	V59 β^-	V60 β^-
Ti50 0+ 5.4	Ti51 5.76 m 3/2- β^-	Ti52 1.7 m 0+ β^-	Ti53 32.7 s (3/2-) β^-	Ti54 0+ β^-	Ti55 β^-	Ti56 0+ β^-	Ti57 0+ β^-	Ti58 0+ β^-	

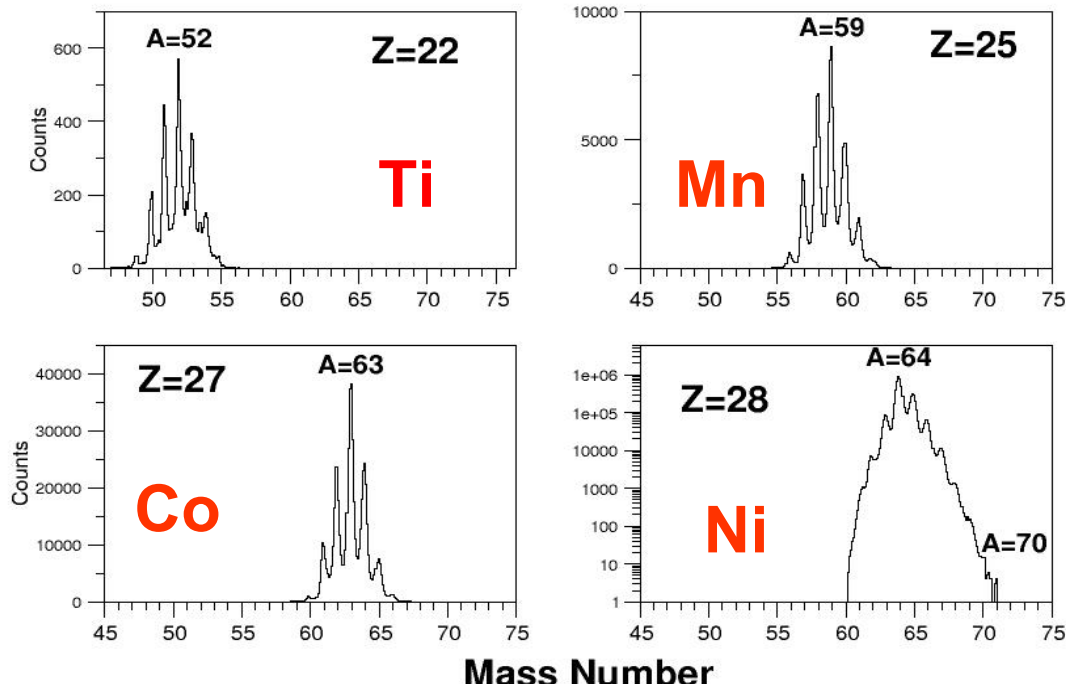
Goal: n-rich A~60 (Cr,Fe & Ti) nuclei, deformation effects in the middle of the $\pi f_{7/2}$ vpf-shell

64Ni 400MeV + 238U

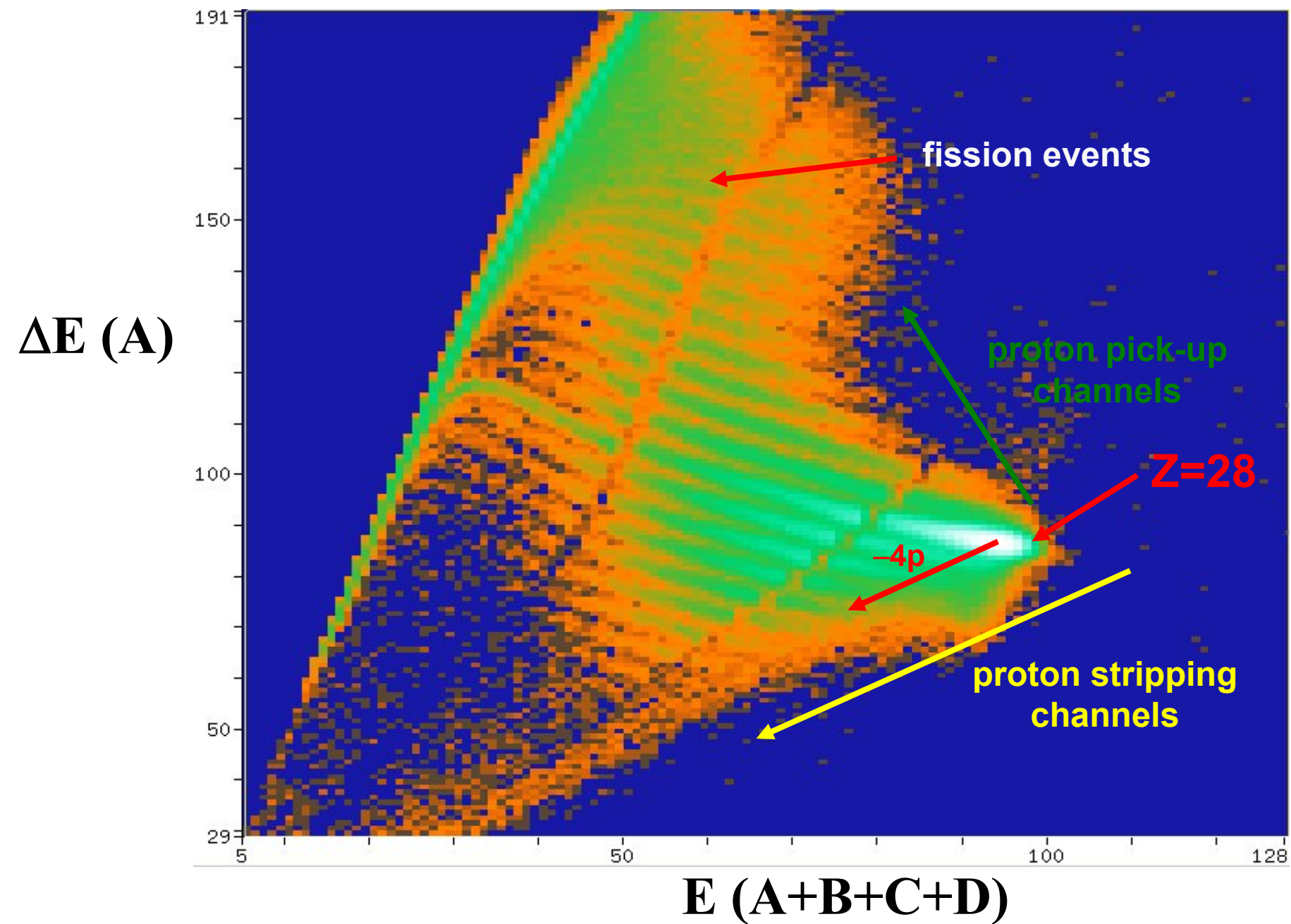
S.M.Lenzi, S.J.Freeman
Analysis: N.Marginean

Preliminary (only 1/2 sorted)

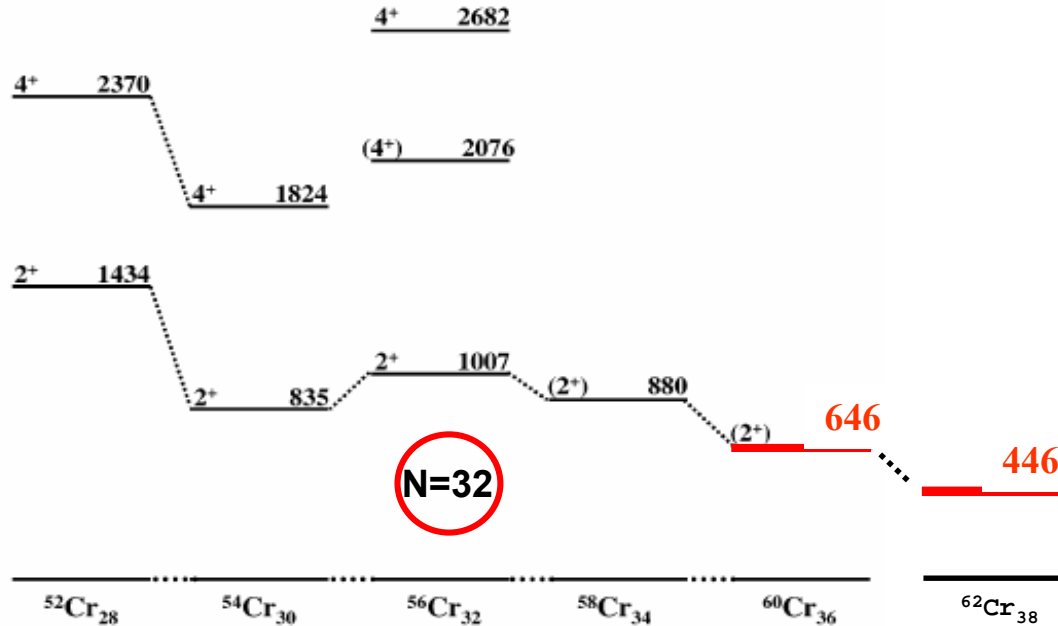
MASS & Z selection



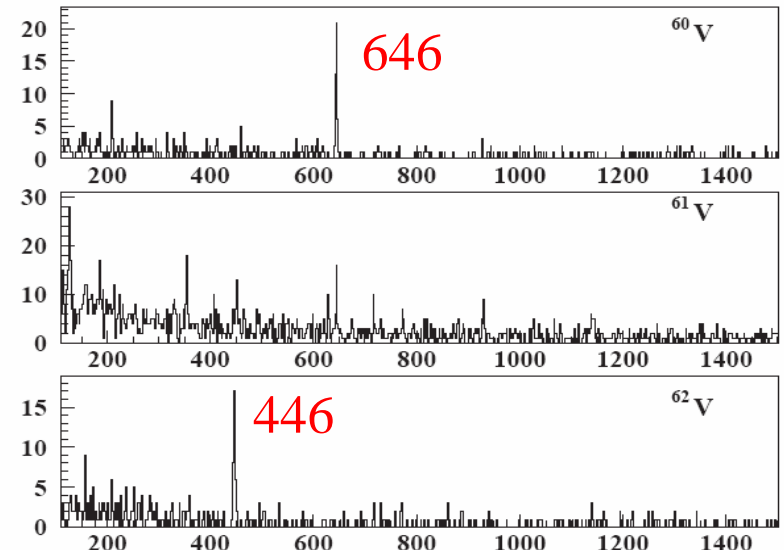
^{64}Ni 400MeV + ^{238}U IC ΔE -E matrix



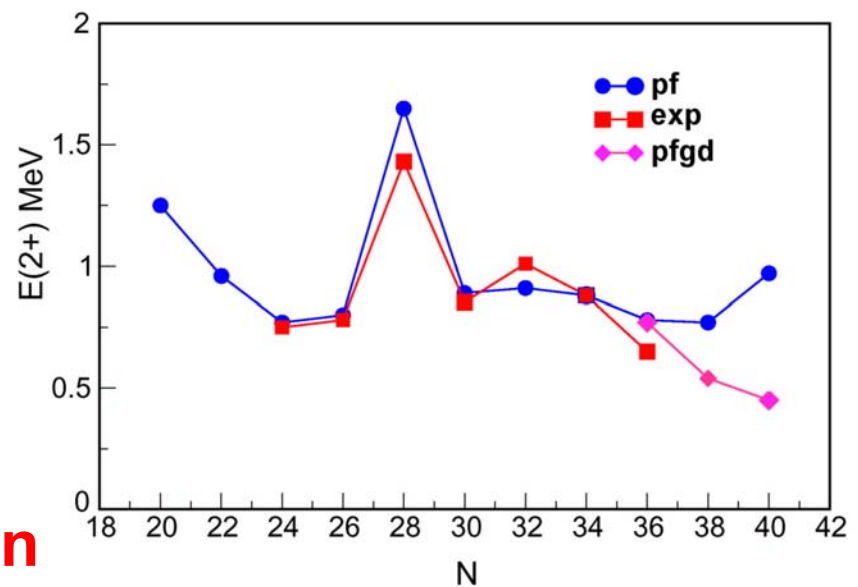
Neutron-rich Cr isotopes with N>32: only the 2⁺ known from β -decay studies



E.Caurier et al.,
Eur. Phys. J. A 15 (2002) 145
LSSM Calculations



GANIL: O.Sorlin et al.,
Eur. Phys. J. A 16 (2003) 55
MSU: P.F.Mantica et al.,
Phys. Rev. C 67 (2003) 014311



N=32 Shell closure: B.Fornal
Onset of deformation N>32: S.Freeman

^{64}Ni 400MeV + ^{238}U

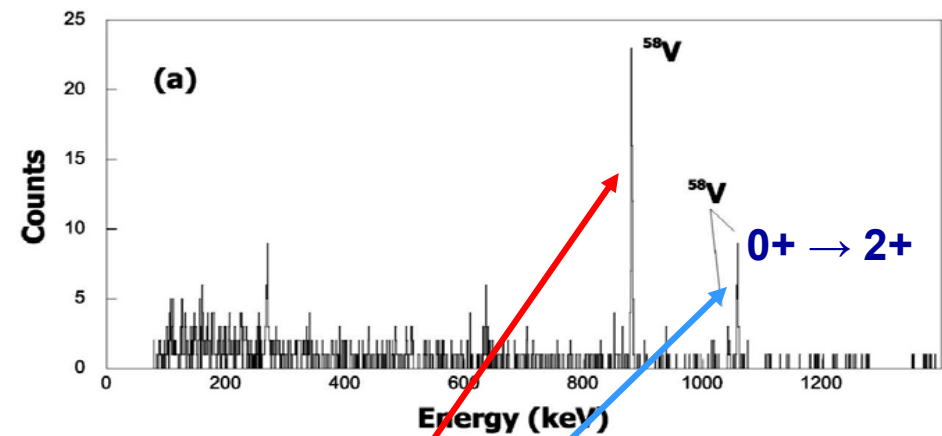
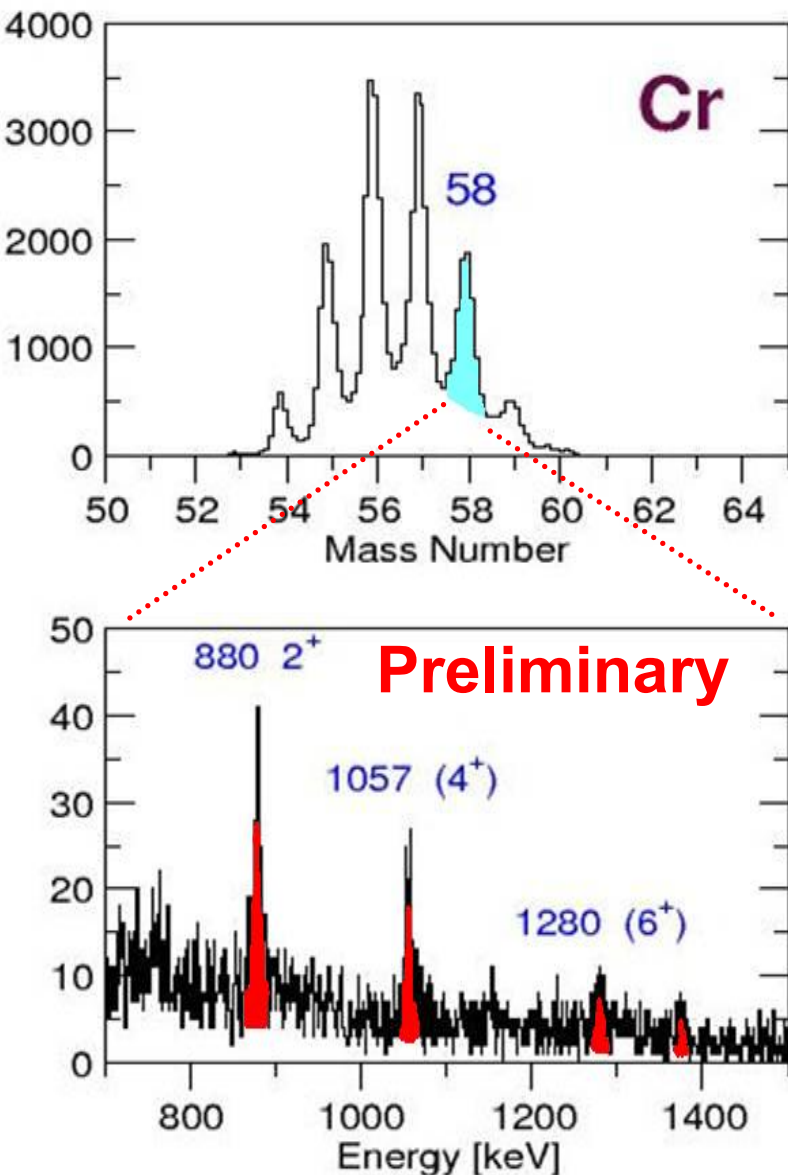


TABLE V. γ rays observed following the decay of ^{58}V .

E_γ (keV)	$\frac{\tau_{abs}}{\tau}$ (%)	Initial state (keV)	Final state (keV)
879.7 ± 0.4	62 ± 7	880	0
1041.2 ± 0.7	8 ± 3		
1056.4 ± 0.5	28 ± 4		
1501.4 ± 0.6	5 ± 2		
1570.6 ± 0.6	5 ± 2		
2216.8 ± 0.7	13 ± 2		

P.F.Mantica et al.,
Phys. Rev. C 67 (2003)014311

From our data the 1056.4 keV transition is the $4^+ \rightarrow 2^+$ member of the yrast cascade. The ^{58}V g.s. is probably 3^+ , also predicted at low energies.

Pure fp shell LSSM calculations reproduce the experimental levels in this slightly deformed nucleus

$$E_{4+}/E_{2+} = 2.20$$

$$E_{6+}/E_{2+} = 3.65$$

58Cr

KB3G

FPD6



— (10⁺) —



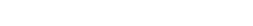
— (8⁺) —



— (6⁺) —



— (4⁺) —



— 2⁺ —

LSSM

EXP.

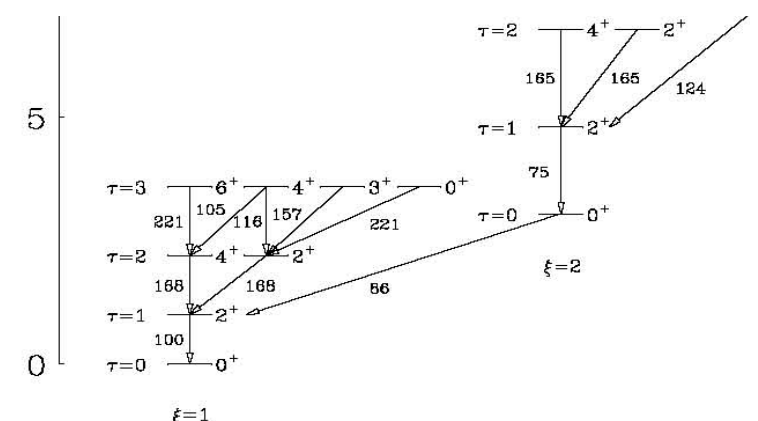
LSSM



E(5) critical point symmetry
vibrator to
 γ -unstable rotor

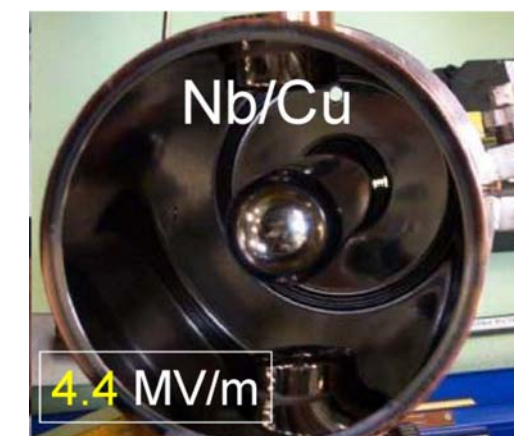
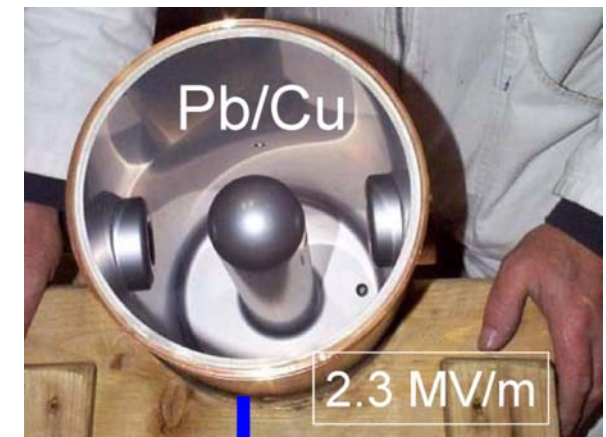
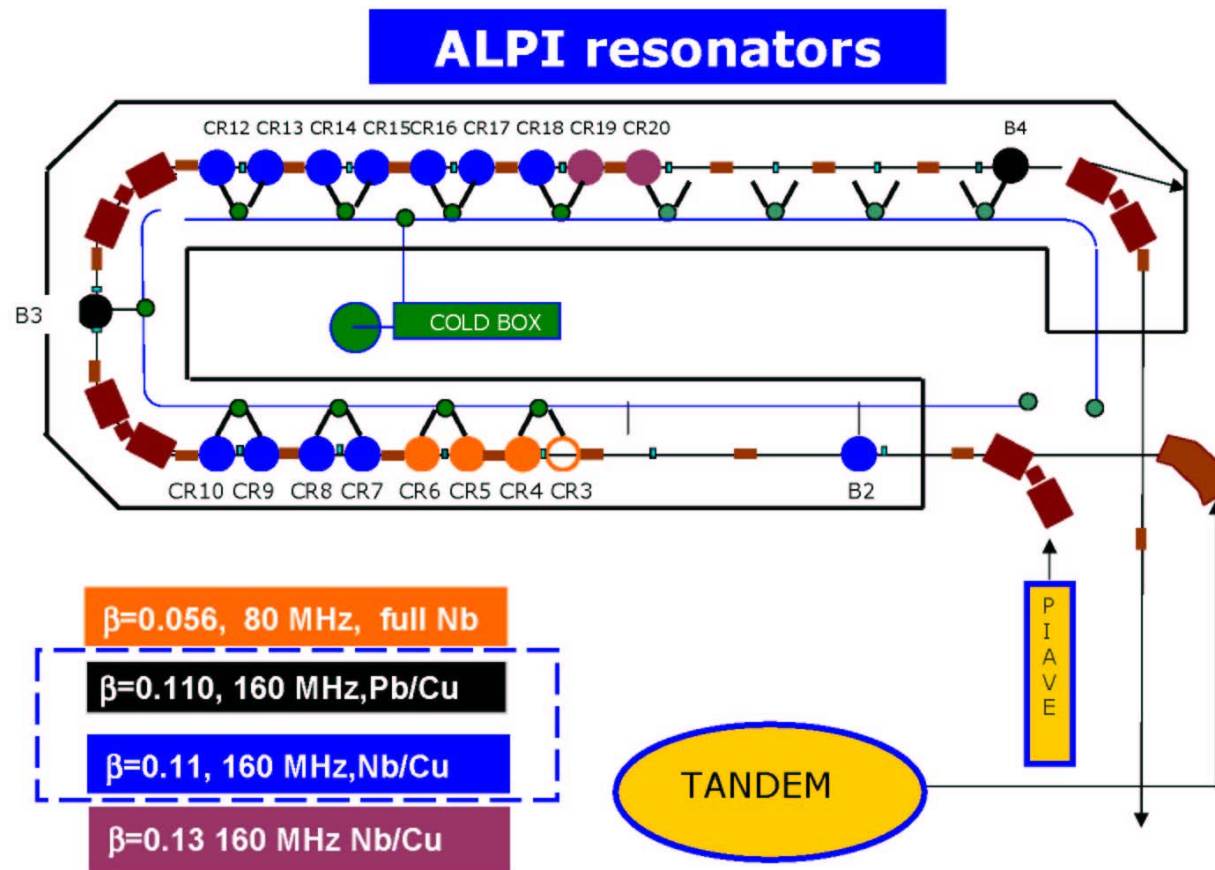
TABLE 1. Excitation energies of the E(5) symmetry.

	$\xi = 1$	$\xi = 2$	$\xi = 3$	$\xi = 4$
$\tau = 0$	0	3.03	7.58	13.64
$\tau = 1$	1	4.80	10.11	16.93
$\tau = 2$	2.20	6.78	12.86	20.44
$\tau = 3$	3.59	8.97	15.81	24.16

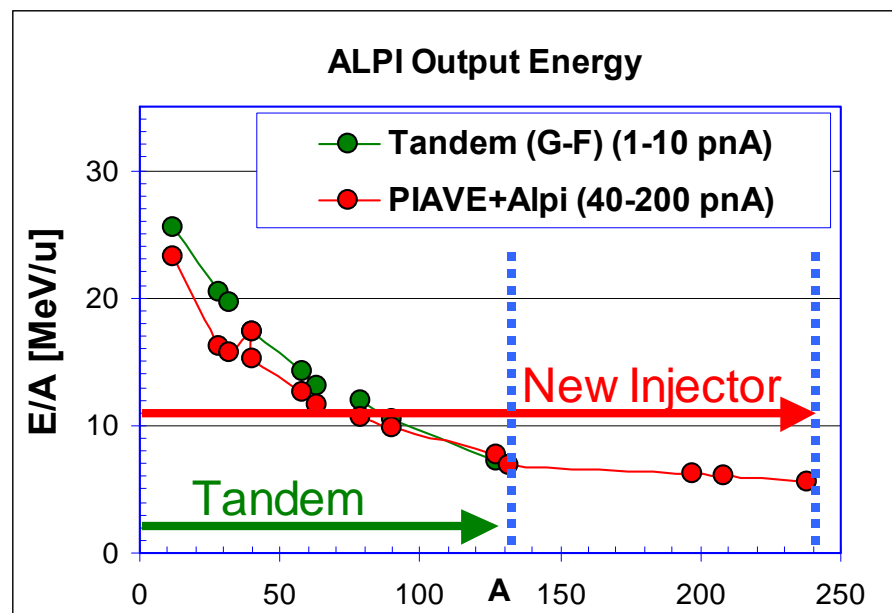
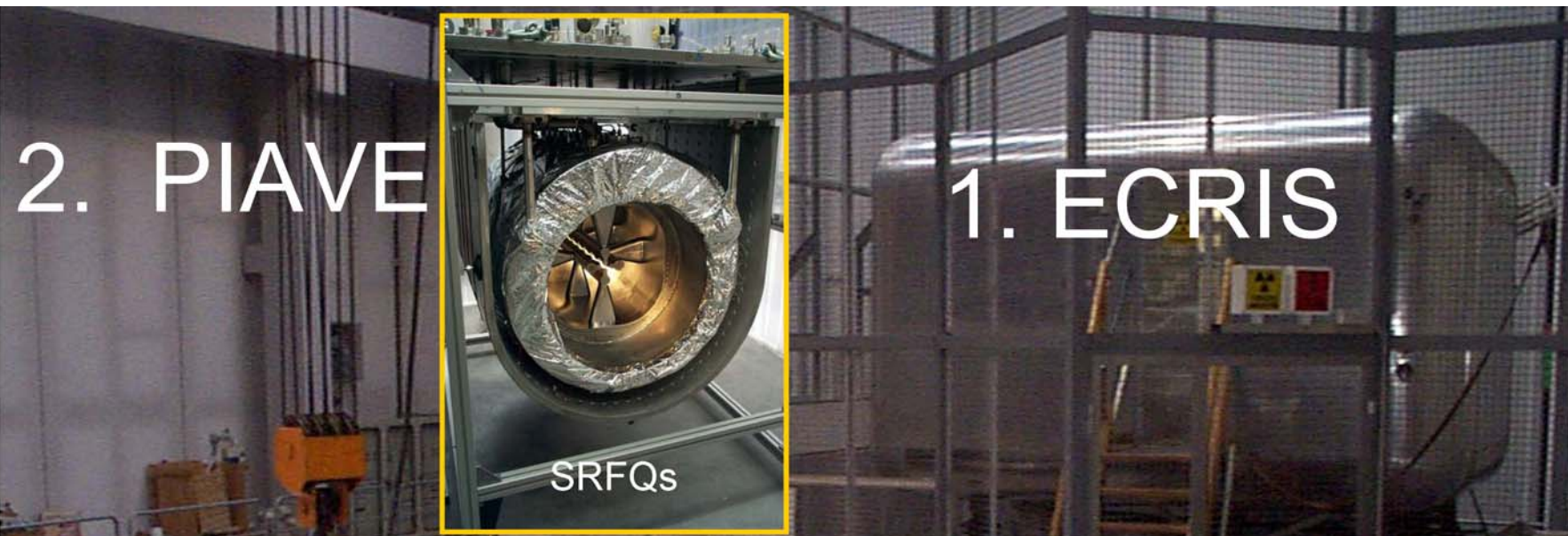


Present at LNL :

Tandem – ALPI beams (therefore Tandem beams) up to A~100. Beam intensities increased up to few pnA (6pnA for 82Se, 4pnA for 90Zr) due to the ALPI energy upgrade (equivalent to ~32MV). Heavier beams available with the low β cavities.



Perspectives:



Positive ion injector ECRIS + PIAVE commissioned with O and Kr beams. Transmission 40%. Ar, Kr and Xe (also Ag and Cu) beams during 2005, program to develop Sn, Cd, Sm and Pb beams at the ECR started

Summary

- The CLARA-PRISMA setup consisting on an array of 25 EUROBALL Clover detectors coupled with the large acceptance magnetic spectrometer PRISMA is installed and fully functional at LNL.
- The first preliminary results show the capabilities of such installation in combination with the stable beam delivered by the LNL Tandem-ALPI complex. In the future with PIAVE-ALPI.
- In a single few days experiment ~50 nuclei could be studied.
- At the present stage of the instrument and for most cases, additional experimental information is required to build the level scheme once the transitions are assigned.
- The first results show how experiments with stable beams and instruments as CLARA-PRISMA can contribute to the study of exotic nuclei

The CLARA-PRISMA collaboration

- France

IReS Strasbourg

GANIL Caen

- U.K.

University of Manchester

Daresbury Laboratory

University of Surrey

University of Paisley

- Germany

HMI Berlin

GSI Darmstadt

- Italy

INFN LNL-Legnaro

INFN and University Padova

INFN and University Milano

INFN and University Genova

INFN and University Torino

INFN and University Napoli

INFN and University Firenze

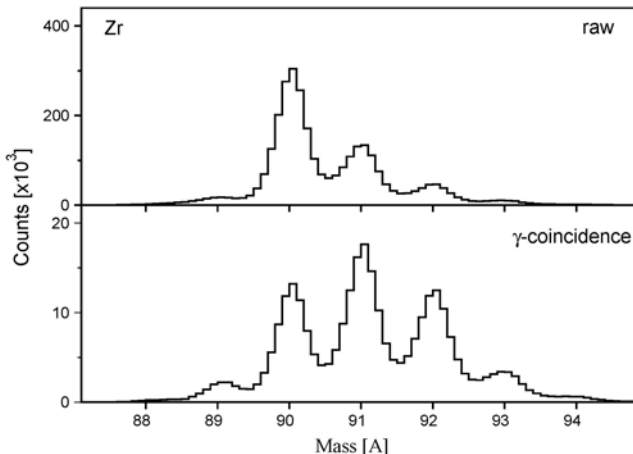
University of Camerino

- Spain

University of Salamanca

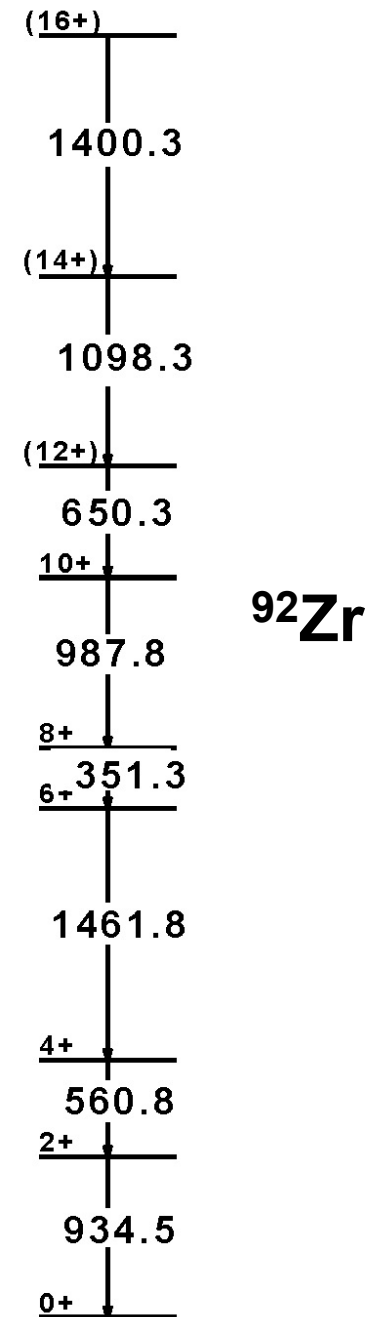
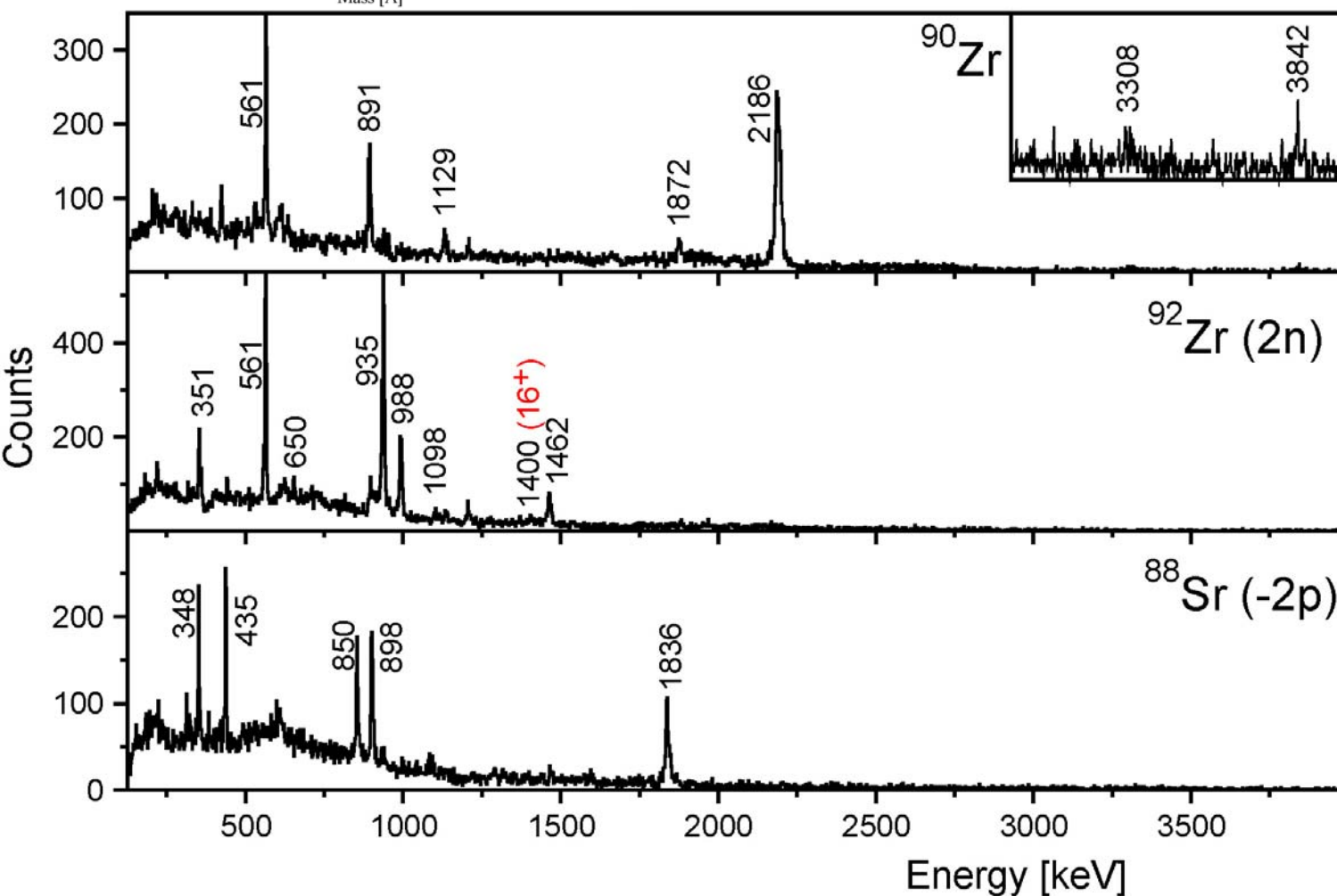
- Romania

Horia Hulubei NIPNE Bucharest

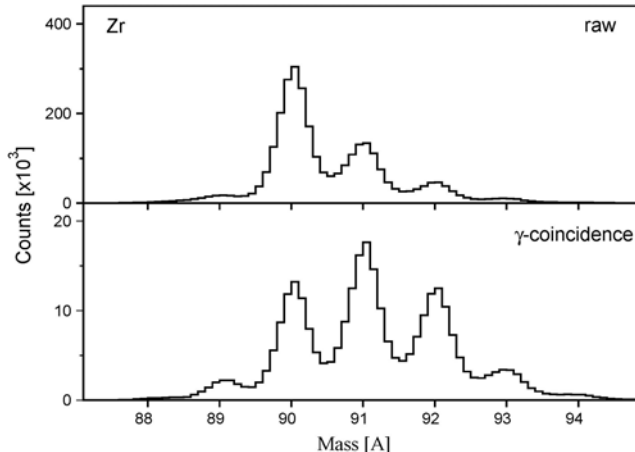


^{90}Zr 560MeV + ^{208}Pb

L.Corradi, C.A.Ur et al.



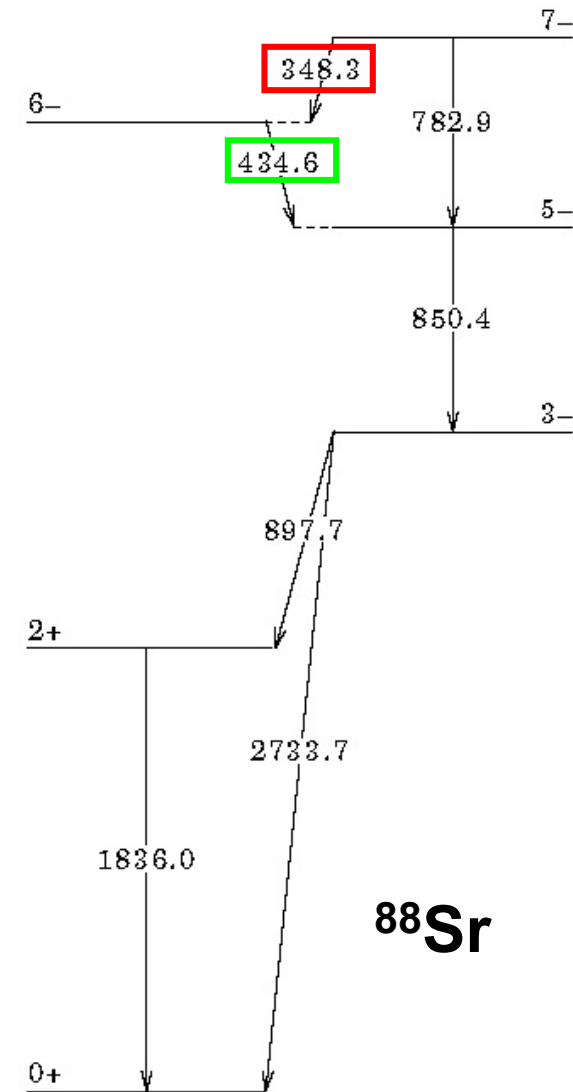
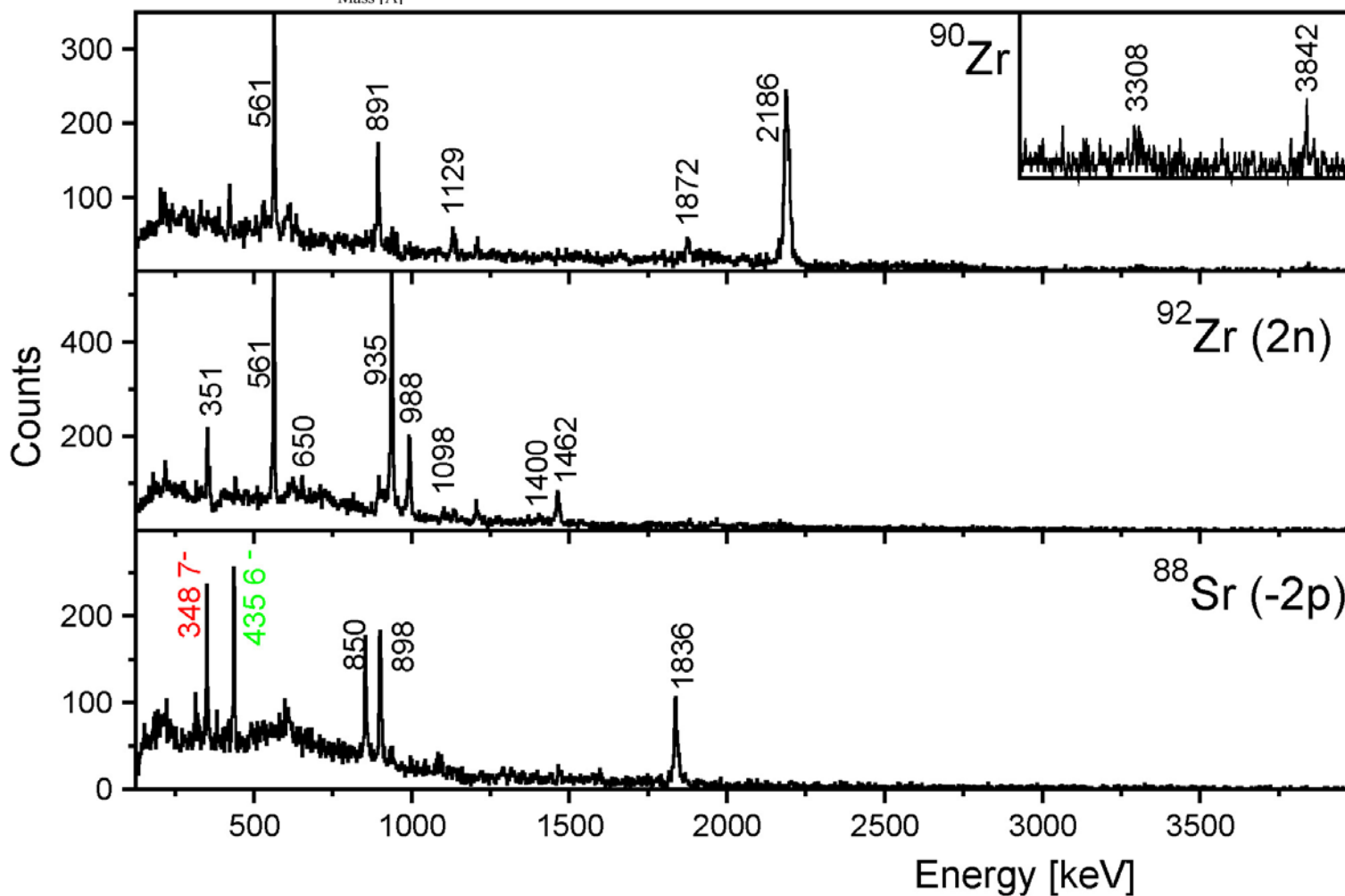
Adopted NNDC
Level Scheme



^{90}Zr 560MeV

+ ^{208}Pb

L.Corradi, C.A.Ur et al.

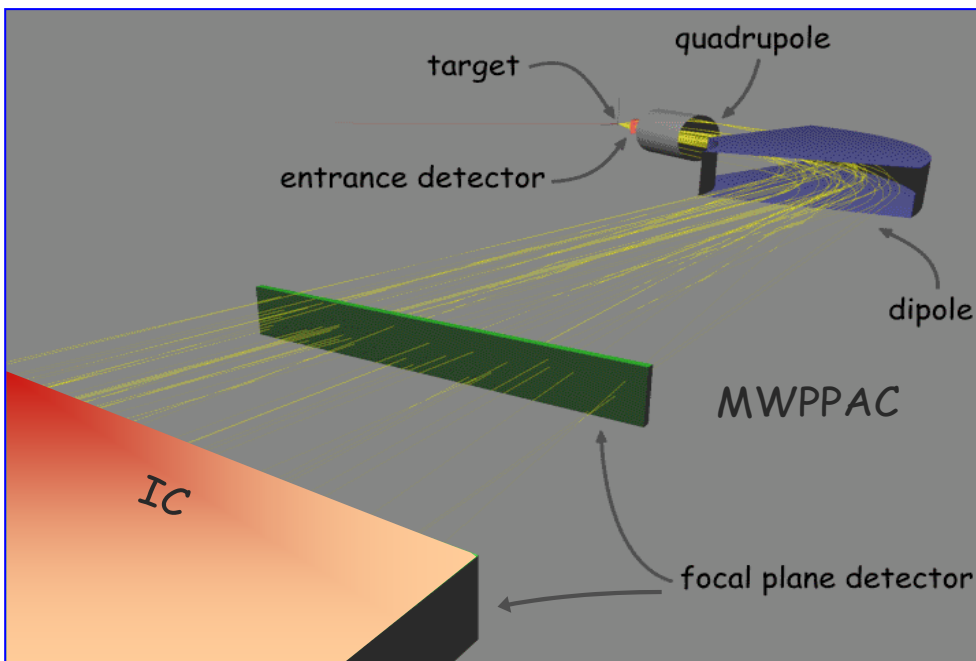


**Adopted NNDC
Level Scheme**

Analysis of PRISMA (CLARA) data

A complete tracking algorithm for PRISMA was developed

Ingredients {
 Entrance detector position (MCP)
 TOF Entrance detector- MWPPAC ($\sim 5\text{m}$)
 Focal Plane position MWPPAC + IC
 Total Energy and Z ($\Delta E/E$) from IC

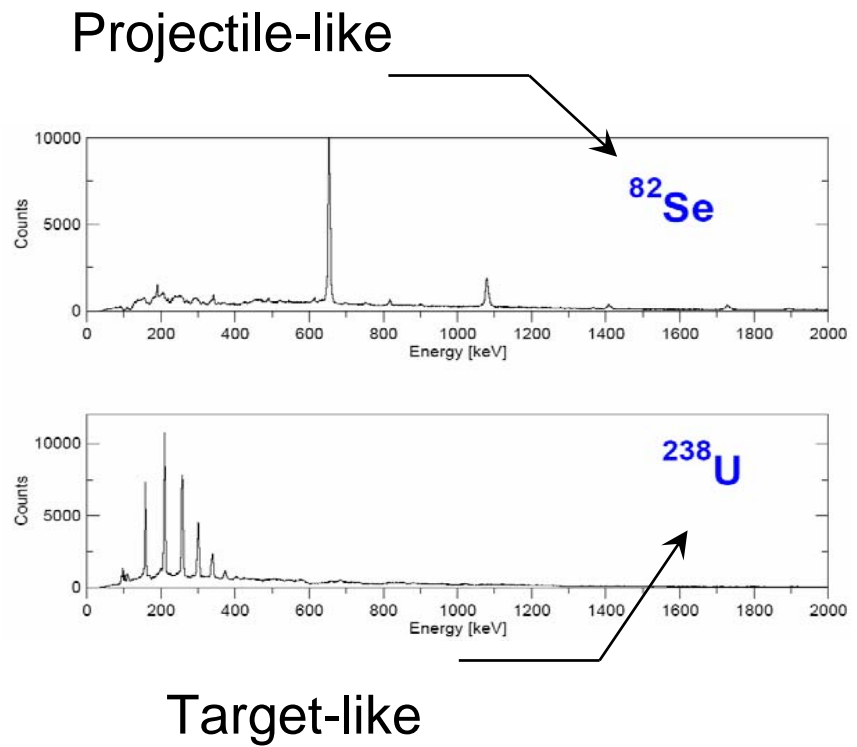
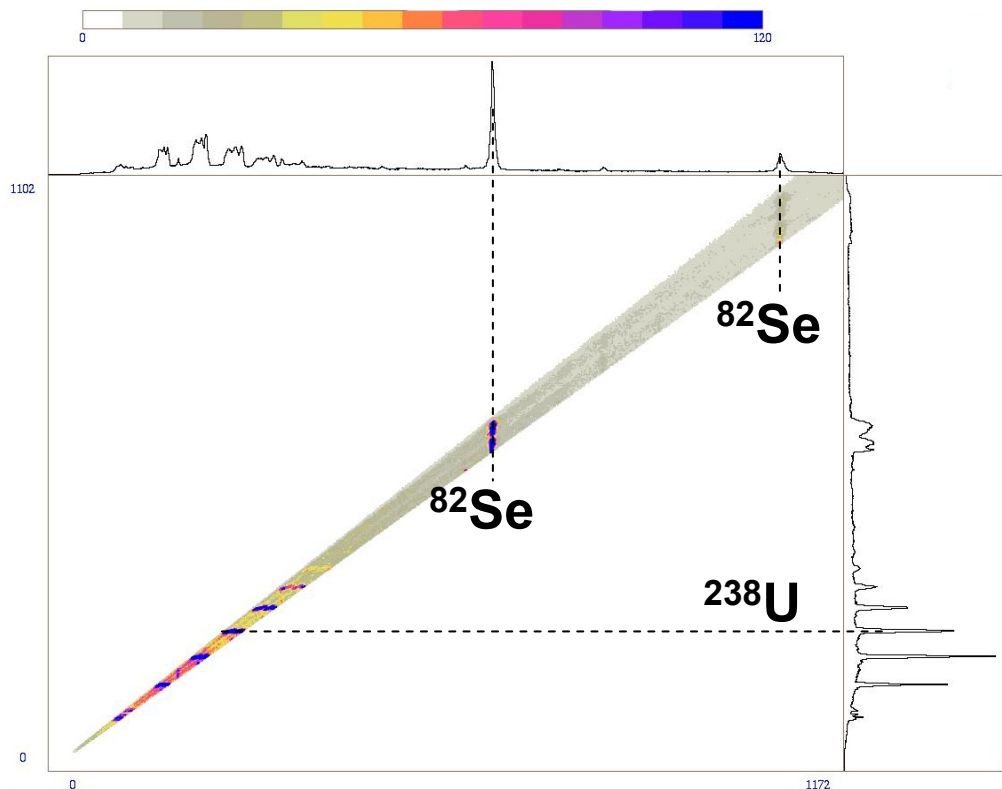


- Doppler correction** {
 - precise position on entrance detector
 - true recoil velocity
- A/q** {
 - trajectory in dipole
- Charge state** {
 - total energy

CLARA Doppler correction

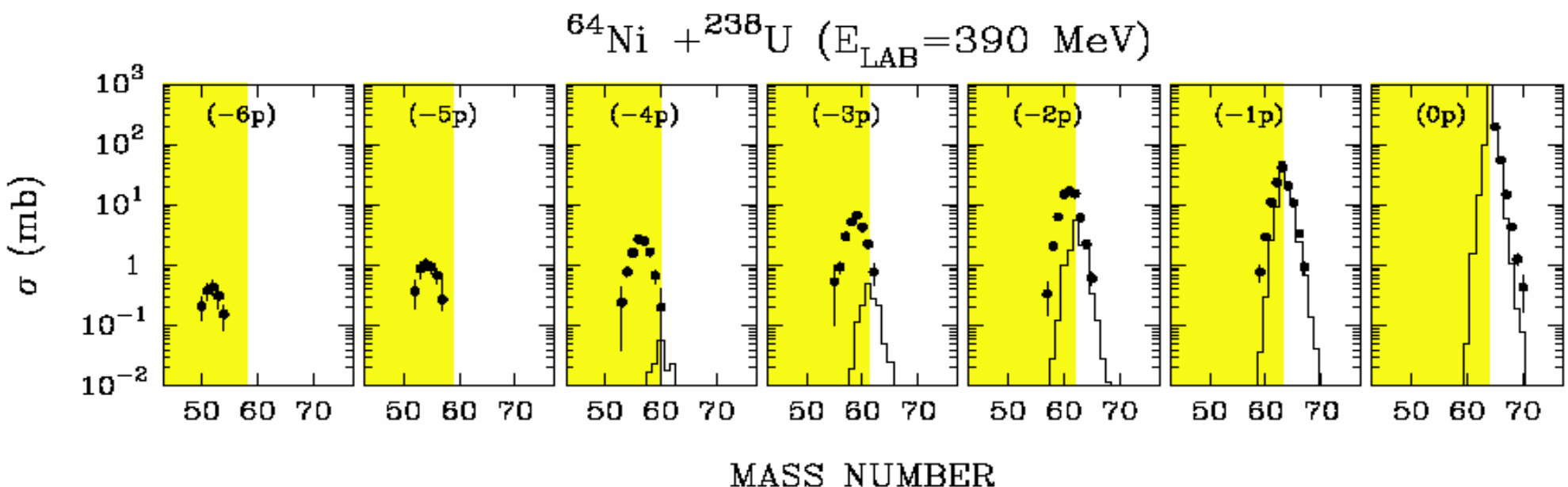
Energy resolution of 1% at recoil velocity v/c = 10%

$^{82}\text{Se} + ^{238}\text{U}$ with ^{82}Se selected in PRISMA



Multinucleon transfer processes in $^{64}\text{Ni} + ^{238}\text{U}$

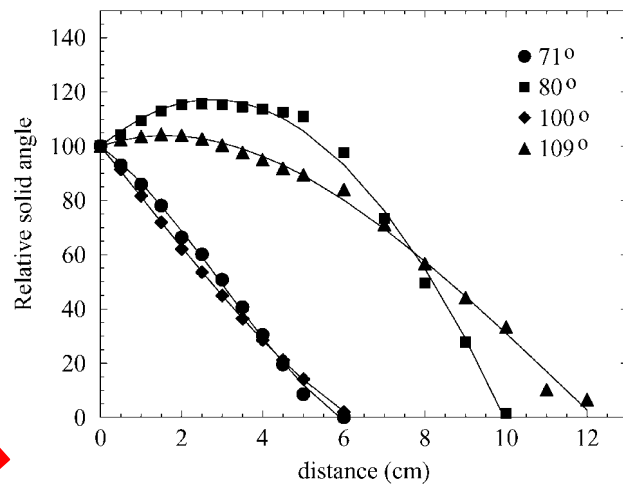
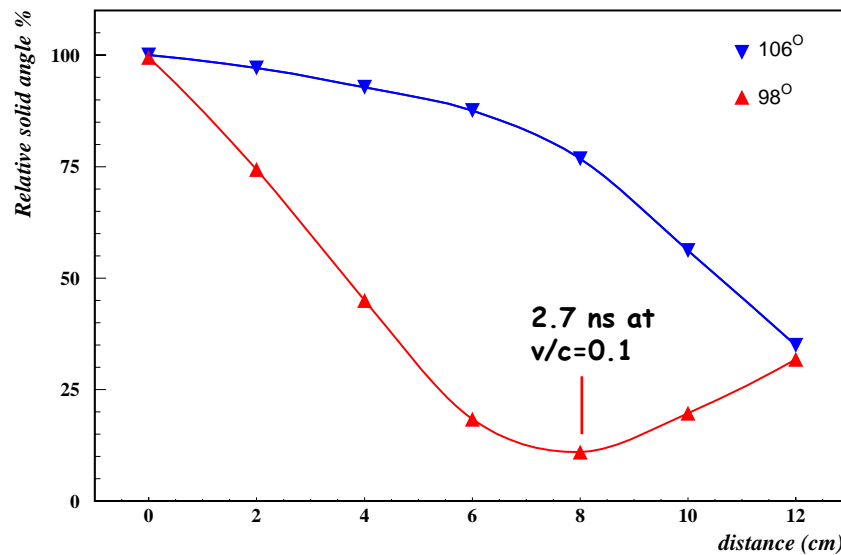
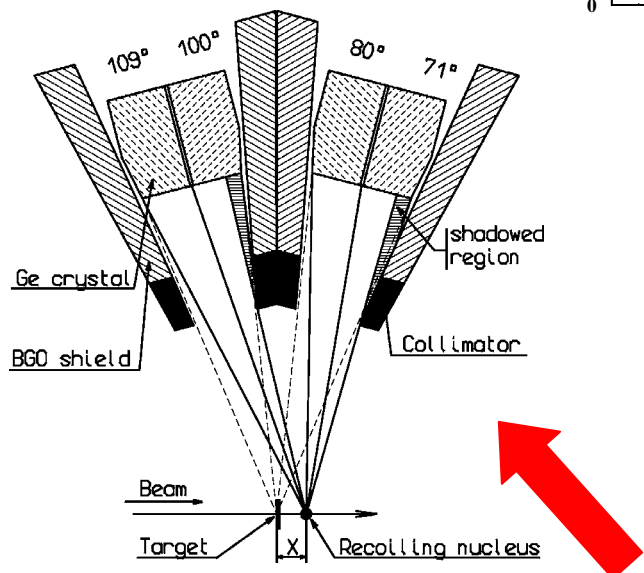
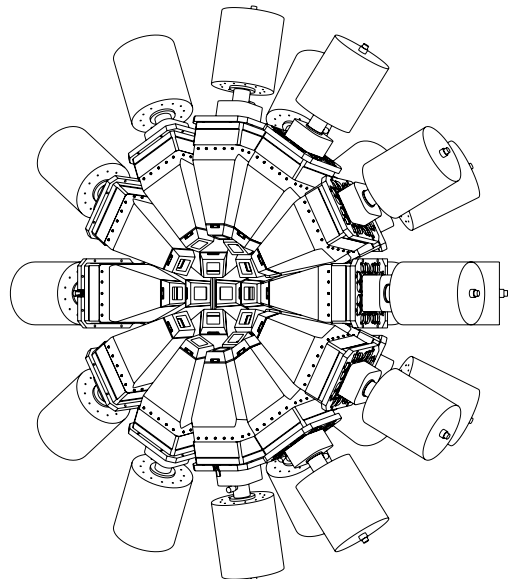
L. Corradi, A. M. Stefanini, and C. J. Lin

Istituto Nazionale di Fisica Nucleare, Laboratori Nazionali di Legnaro, Via Romea 4, I-35020 Legnaro, Padova, Italy

Lifetime measurements with the Clover array at Prisma

- Recoil Shadow anisotropy method:
Based on the array-collimator geometry.
Lifetimes ranging from ~0.5 to ~20 ns.
E.Gueorguieva et al. NIM A 474 (2001) 132.
- Differential Plunger method (to be developed):
Needs a degrader foil at different distances from target.
Lifetimes ranging from ~1 ps to ~1 ns.
- RFD method:
Developed at the Krakow Recoil Filter Detector.
Based on the line shape analysis of the Doppler shifted lines
and the change of momentum introduced by the straggling of the
products in the target.
Needs an accurate position sensitive detector as the PRISMA
start MCP .
Lifetimes ranging from ~50 fs to ~1 ps.
P.Bednarczyk, W.Meczynski, J.Styczen et al.

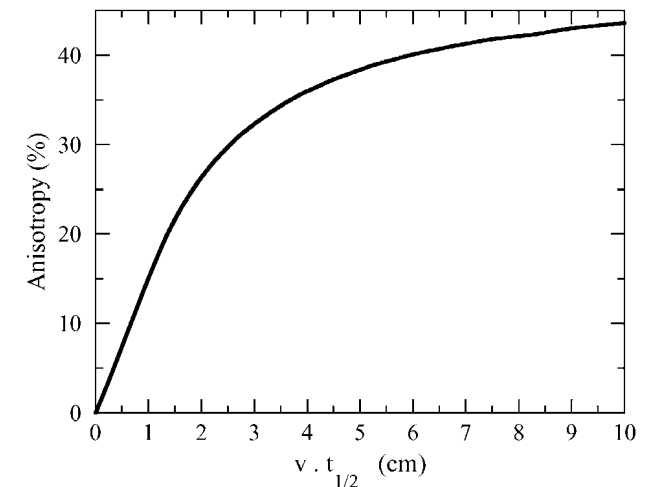
Recoil Shadow Anisotropy Method



Angles for the Ge crystals of the Clover array ring:

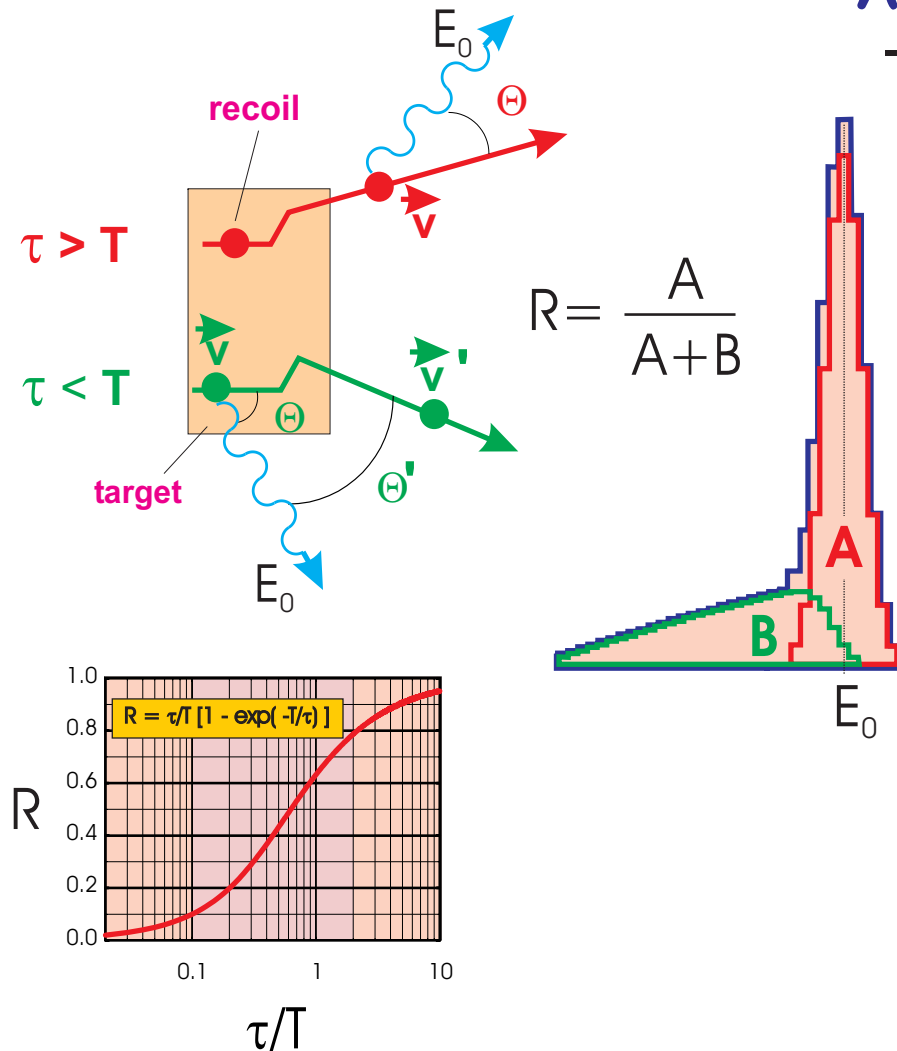
$$\theta = 106^\circ$$

$$\theta = 98^\circ$$



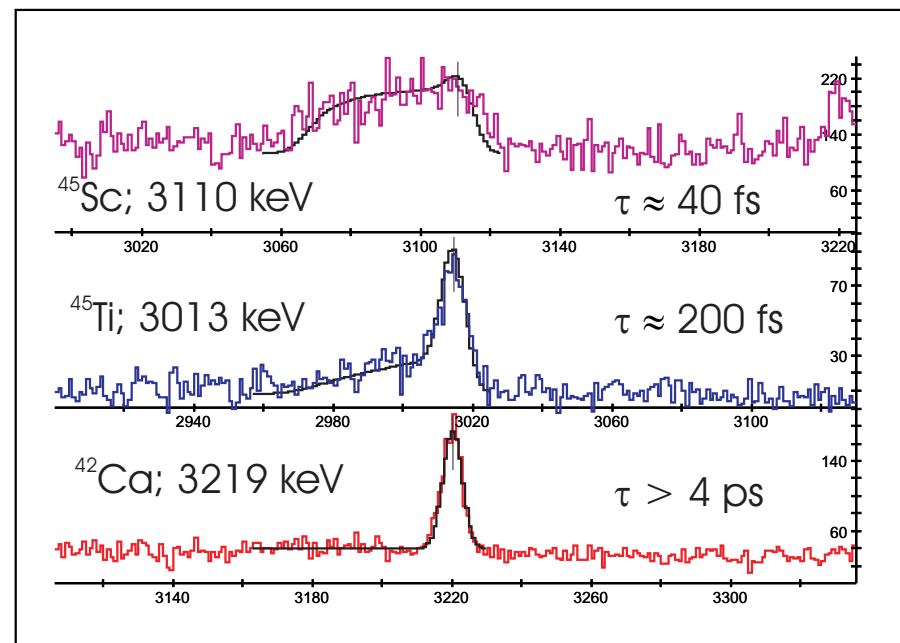
For EUROBALL: E.Gueorguieva et al. NIM A 474 (2001) 132

A short lifetime determination with RFD



The range of measured lifetimes can be chosen by a selection of the target thickness.

68MeV $^{18}\text{O} + 0.8\text{mg/cm}^2$ ^{30}Si ;
Recoil transit time ≈ 0.4 ps



In the measurement τ ranging from 40 to 800 fs could be determined.